

BENCHMARK MANUAL

Altair Manufacturing Solver: Casting Benchmark Manual

CASTING BENCHMARK MANUAL

Solidification Tests

1.1. Temperature analysis during solidification using constant heat transfer rate

Objectives

The present test, based by the results obtained by the reference work (Kron et al. 2017) is carried out with the purpose of evaluating the modelling predictions regarding the solidification process. To this aim, the temperatures of the casting and other components have been measured during solidification. This test presents the first approach to the modelling predictions as it is set up with ideal boundary conditions where the heat transfer coefficient is selected as constant. By doing the benchmark with pure heat transfer calculations (HTC constant) it is possible to do a preliminary comparison between the assumptions considered by the different solvers while developing the code.

Method and Description

This test aims to measure the temperature curves during solidification in four different elements: cast, mold, core and insulation. To replicate the experiment carried out by the authors (Kron et al. 2017) we consider the geometry shown in Figure 1, which consists in a series of concentric cylinders.

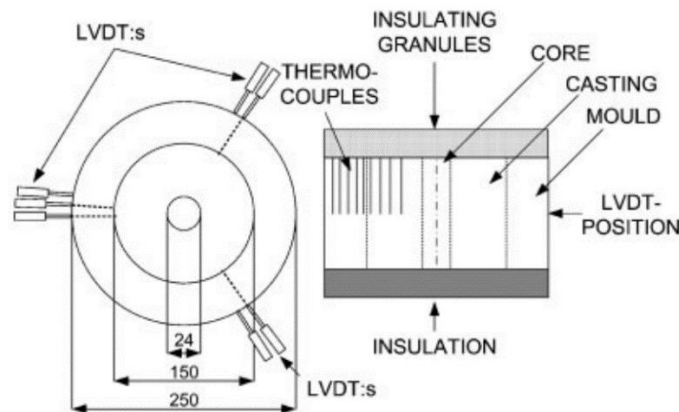


Figure 1. Geometry of the experimental Set-up for the temperature analysis (Kron et al. 2017).

The height of the mold is 100mm and the diameters are 24, 150 and 250 mm, respectively.

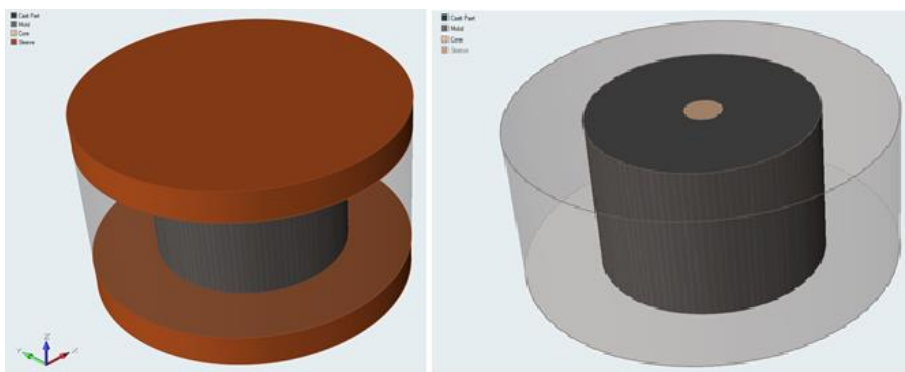


Figure 2. Geometry of the Inspire Cast simulation.

Parameters

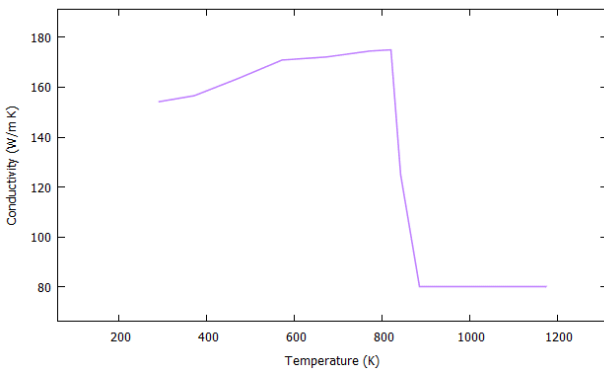
MATERIAL DETAILS

The numerical simulations in this experiment consider four different material domains whose properties are described in this section.

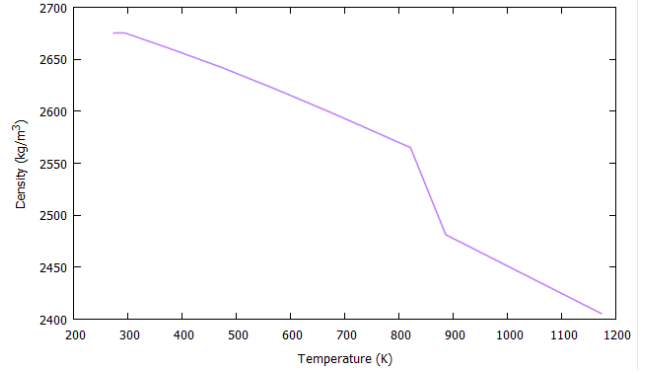
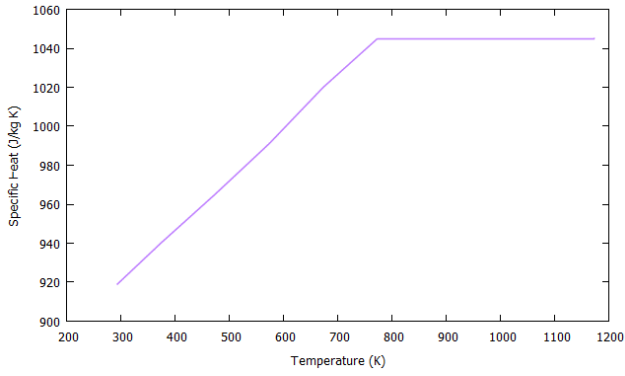
As outer thermal boundary condition the HTC considered is $HTC_{OUT}=20 \text{ Wm}^{-2}\text{K}^{-1}$. This parameter is constant and assumed between components in contact with the surroundings (mold and insulation). This is an unrealistic condition, but it enables to do a basic comparison between the codes of the simulation softwares.

The alloy chosen for the cast part is Al-7%Si-0.3%Mg (A356) with an estimated initial temperature after filling of 989.15K. The **latent heat of this alloy is 431 kJ/kg**. HTC between part and mold is constant with value $HTC_{Part-Mold}=898 \text{ Wm}^{-2}\text{K}^{-1}$. Likewise, HTC between part and core is constant but with value $HTC_{Part-Core}=2000 \text{ Wm}^{-2}\text{K}^{-1}$.

The remaining material properties follow the curves describe in the figures and tables below.

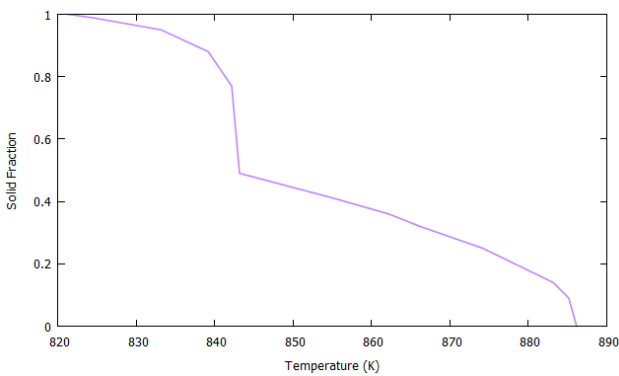


Temperature (K)	Thermal Conductivity (W/m K)
293.14	154.20
293.15	154.20
373.15	156.60
473.15	163.50
573.15	170.90
673.15	172.10
773.15	174.50
824.15	168.18
833.15	147.73
839.15	134.09
842.15	127.27
843.15	125.00
850.15	117.67
855.15	112.44
862.15	105.12
866.15	100.93
874.15	92.58
883.15	83.14
885.15	81.05
1173.15	80.00
1173.16	80.00



Temperature (K)	Specific heat (J/kg K)
293.14	919.00
293.15	919.00
373.15	940.00
473.15	965.00
573.15	991.00
673.15	1020.00
773.15	1045.00
821.15	1045.00
886.15	1045.00
1023.15	1045.00
1173.15	1045.00
1173.16	1045.00

Temperature (K)	Density (kg/m ³)
273.14	2675.00
273.15	2675.00
293.15	2675.00
373.15	2661.00
473.15	2642.00
573.15	2621.00
673.15	2599.00
773.15	2576.00
821.15	2565.00
886.15	2481.20
1023.15	2445.00
1173.15	2405.40
1173.16	2405.40



Temperature (K)	Solid Fraction
821.15	1.00
821.15	1.00
824.15	0.99
833.15	0.95
839.15	0.88
842.15	0.77
843.15	0.49
855.15	0.41
862.15	0.36
866.15	0.32
874.15	0.25
883.15	0.14
885.15	0.09
886.15	0.00
886.15	0.00

The mold is made from a low alloy steel with composition 0.14%C, 0.35%Si and 1.2%Mn. The initial temperature of the mold is 403.15K.

Mold Properties	
Density	7800 kg/m ³
Specific Heat	544 J/(kg K)
Conductivity	45.29 W/(m K)

The core is a quartz tube filled with oil bound sand, but it is modelled using exclusively sand properties. It has initial temperature 403.15K.

Core Properties	
Density	1500 kg/m ³
Specific Heat	800 J/(kg K)
Conductivity	0.9 W/(m K)

The insulation component covers the region above and below the whole set. Therefore, it is in direct contact with mold, part and core. The heat transfer coefficient with all components is fixed at $HTC_{All-Insulation}=400 \text{ Wm}^{-2}\text{K}^{-1}$. To simulate the insulation, both parts are designated as sleeves with the properties above described, very low conductivity and with constant density.

Insulation Properties	
Density	1000 kg/m ³
Specific Heat	1760 J/(kg K)
Conductivity	0.1 W/(m K)

MESH

To obtain accurate results when collecting the data from the different points of interest it is crucial to do a right meshing of the model.

In this case, as the measurements are obtained from the different components the mesh must be fine and homogeneous. Table 5 shows the element size for each component in the simulation. This configuration creates a grid with, at least, 250 000 elements in the liquid part. Low conductivities in components as the sleeves creates steep temperature gradients that require a fine mesh to capture results with accuracy.

The mesh details provided in this document correspond to the upper limit to element size in order to ensure good results. Coarser mesh does not improve considerably processing time and result in inaccuracies.

Component	Size
Cast Part	3.0 mm
Mold	3.0 mm
Core	3.0 mm

Results

The data is collected in certain points according to the experimental description of Kron et al. (Kron et al. 2017). Considering the mid-height region (50mm) the temperature curve is measured at five different radii as shown in the following table.

Component	Radius
Core	8 mm
Cast Part	45 mm
	69 mm
Mold	77 mm

We proceed to compare the results of the *AMS solver* simulation to the data available in the literature of reference for each component. This includes a comparison between *Casts-Spand3D*, *MagmaSoft*, *Procast* and *Thercast*. Experimental data is also considered for certain regions ($r=69$ and 77 mm).

In Figure 3 is shown that the results obtained with the different simulation solvers are very similar to each other. For the core (a), Thercast is the one that differs the most while AMS solver follows the general tendency. These results are extendable to the following measurements.

Experimental temperatures present some differences with all the calculated temperatures because of the constant HTC restriction considered in the simulation softwares. Overall, the simulations follow very similar behaviors, achieving good results with the assumptions considered in each model.

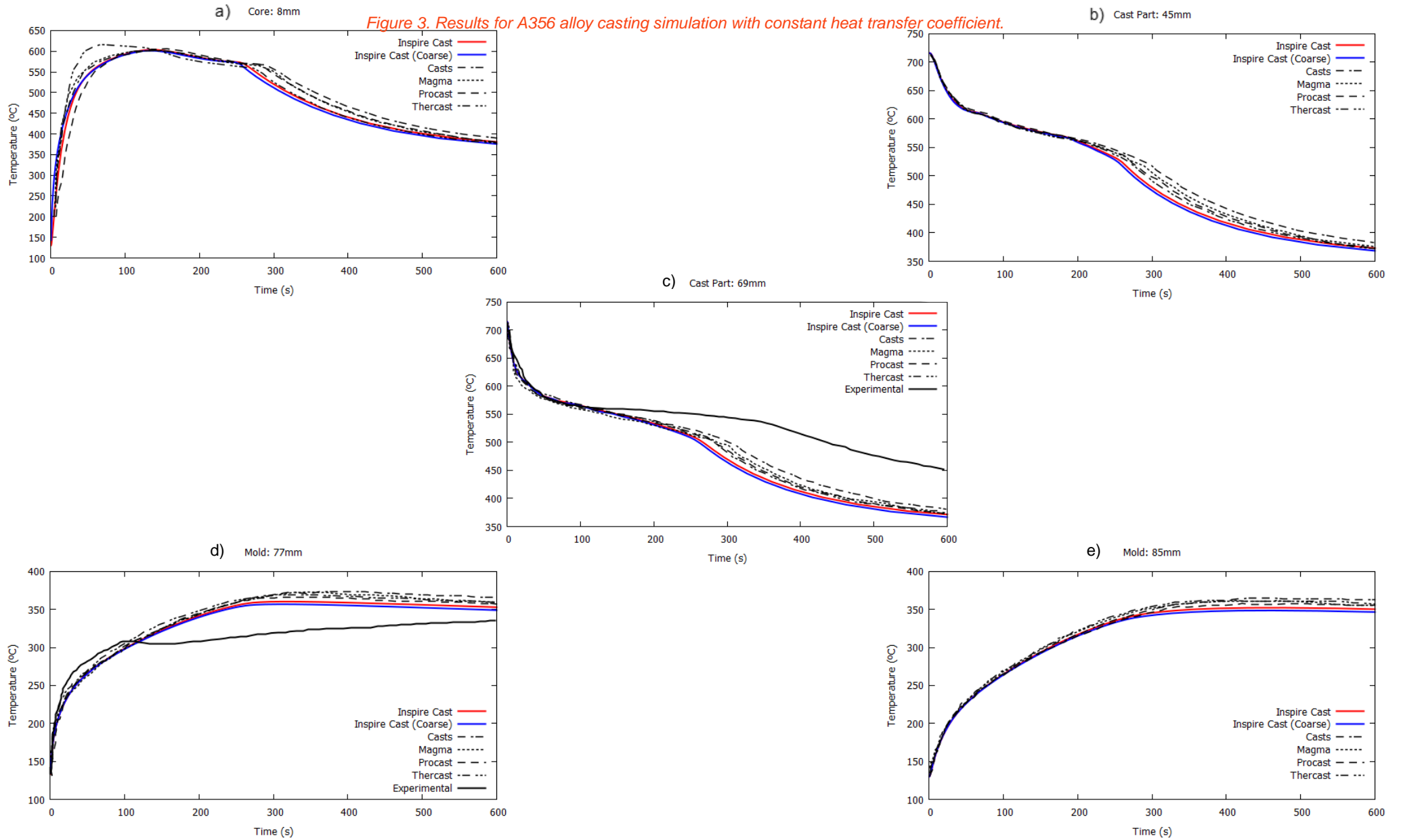
COARSE MESH

In this section, a coarser mesh is considered to run the same experiment. The new mesh has an element size of 6 mm, this corresponds to the double of the size of the previous test (see Figure 4). As shown in Figure 5, the results obtained when enlarging element size are less symmetric and precise.

An element size of such dimensions hinders accuracy, moving the result away from the more realistic solution. The loss of symmetry is an important observation in this case as the geometry is totally symmetric, therefore, such result is due to the deviations related solving the problem by considering large elements.

This example is very illustrative to observe importance of mesh definition in relation of the needs and expectations when running a test and it also shows that, in despite all, results remain good and temperature measurements do not deviate further than 5°C .

Figure 3. Results for A356 alloy casting simulation with constant heat transfer coefficient.



Coarse Mesh

Fine Mesh

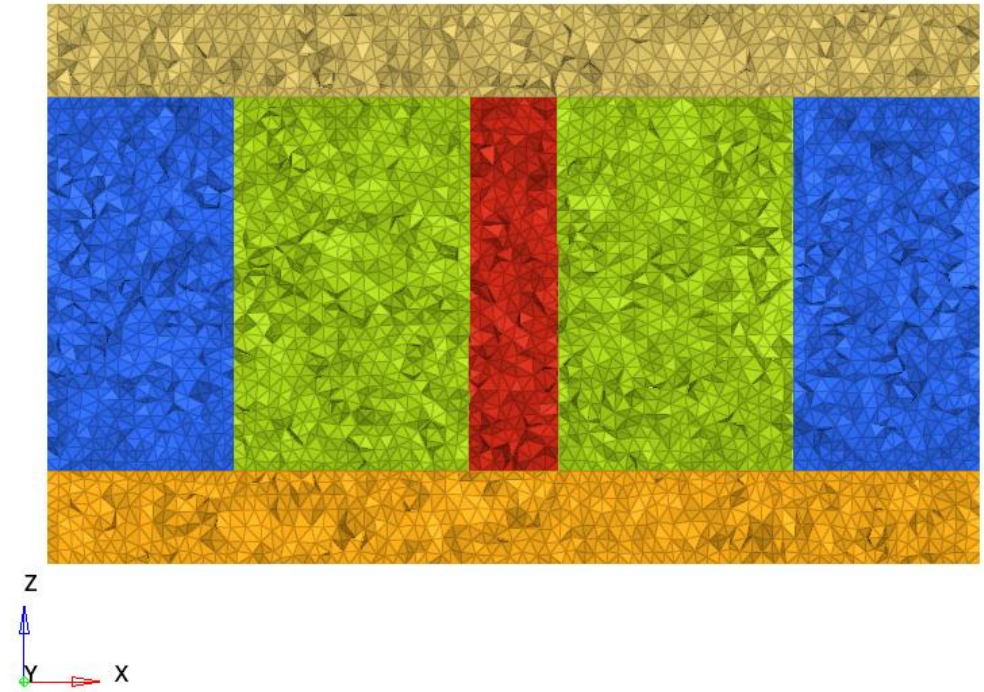
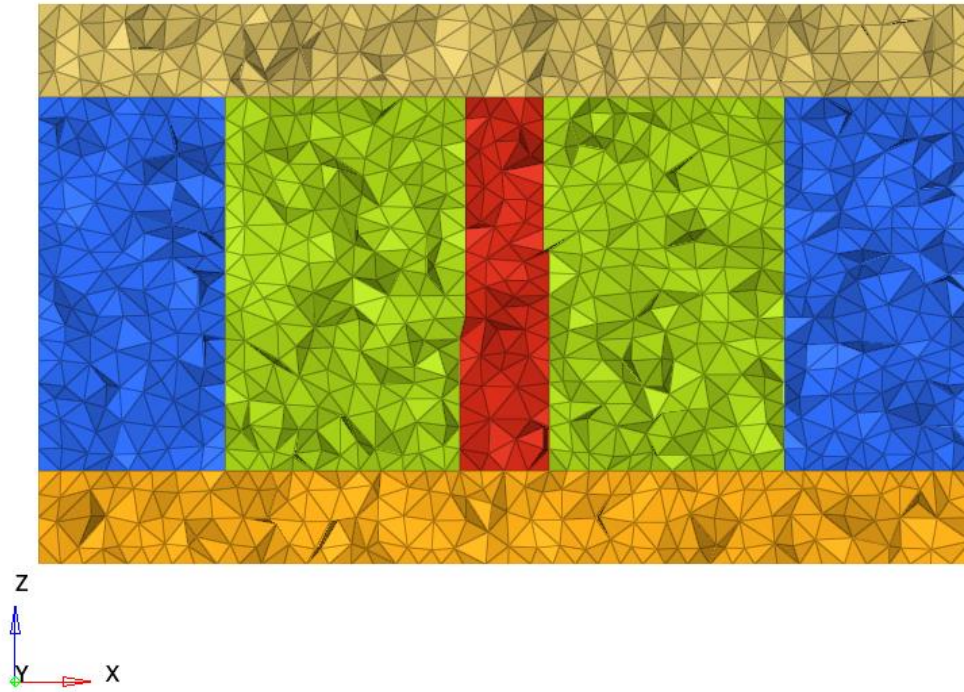


Figure 4. Mesh details: left) coarse mesh ; right) fine mesh.

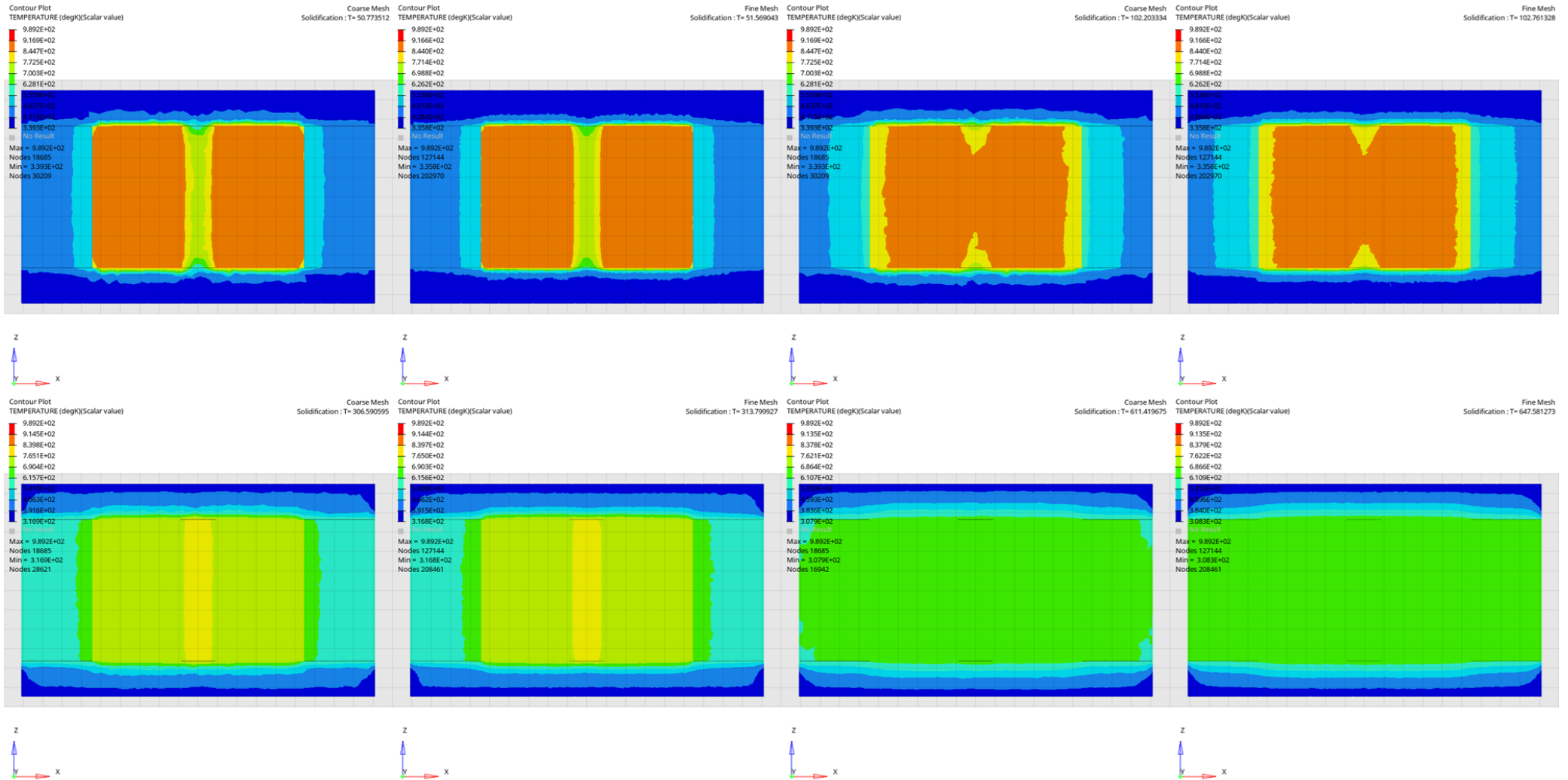


Figure 5. Temperature evolution during solidification (left - coarse mesh ; right - fine mesh) .

1.2. Temperature analysis during solidification using variable heat transfer rate

Objectives

The present test, based by the results obtained by the reference work *Kron et al.*, is carried out with the purpose of evaluating the modelling predictions regarding the solidification process. To this aim, the temperatures of the casting and other components have been measured during solidification and compared to experimental results and another simulation softwares.

Method and Description

This test aims to measure the temperature curves during solidification in four different elements: cast, mold, core and insulation. To replicate the experiment carried out by J. Kron (Kron et al. 2017) we consider the geometry shown in Figure 6, which consists in a series of concentric cylinders.

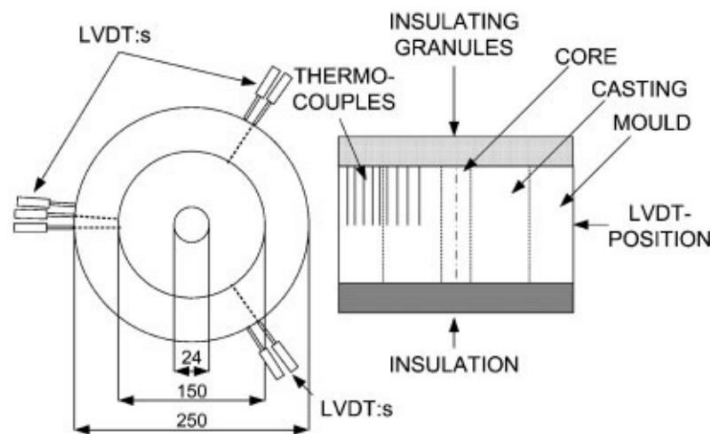


Figure 6. Geometry of the experimental Set-up (Kron et al. 2017).

The height of the mold is 100mm and the diameters are 24, 150 and 250 mm, respectively.

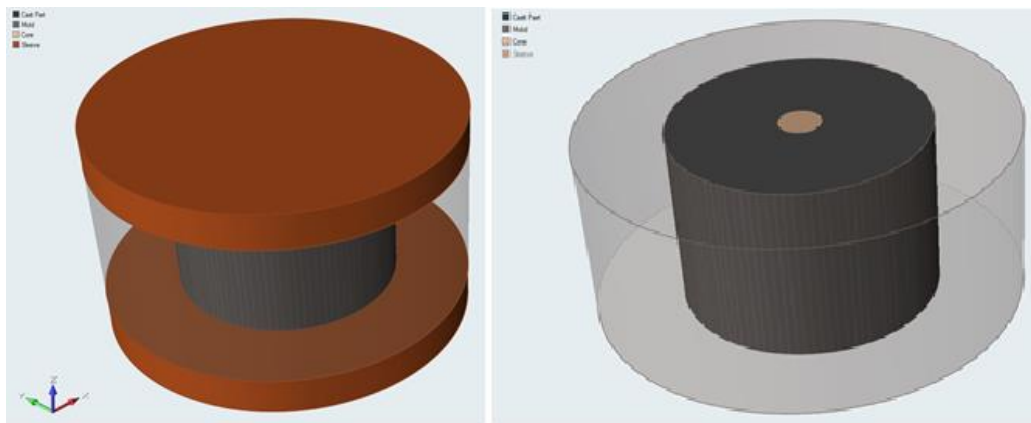


Figure 7. Geometry of the Inspire Cast simulation.

Parameters

MATERIAL DETAILS

The numerical simulations in this experiment consider four different material domains whose properties are described in this section.

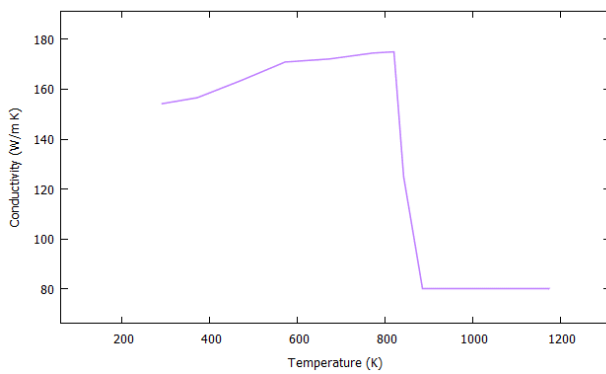
As outer thermal boundary condition the HTC considered is $HTC_{OUT}=20 \text{ Wm}^{-2}\text{K}^{-1}$. This parameter is constant and assumed between components in contact with the surroundings (mold and insulation). This is an unrealistic condition, but it enables to do a basic comparison between the codes of the simulation softwares.

The alloy chosen for the cast part is Al-7%Si-0.3%Mg (A356) with an estimated initial temperature after filling of 989.15K. The **latent heat of this alloy is 431 kJ/kg**. HTC between part and mold is constant with value $HTC_{Part-Mold}=898 \text{ Wm}^{-2}\text{K}^{-1}$. Likewise, HTC between

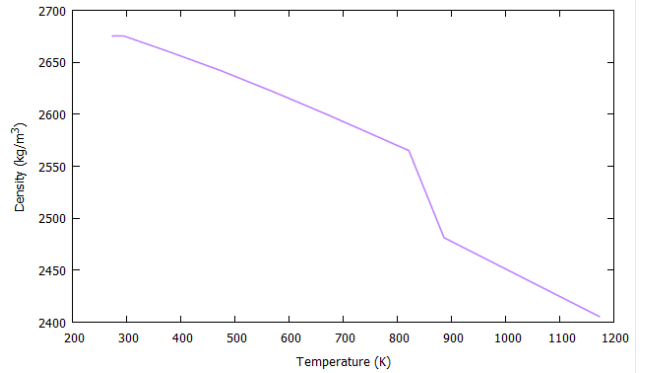
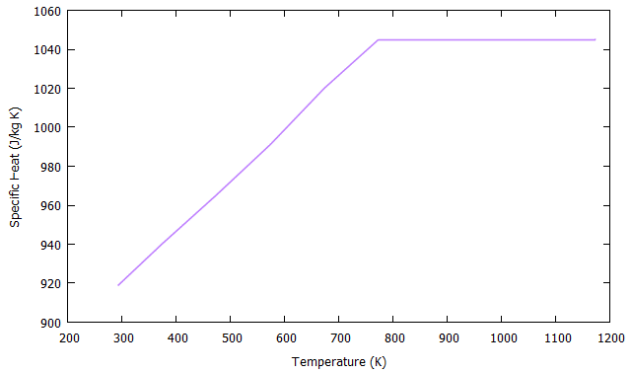
part and core is constant but with value $HTC_{Part-Core} = 2000 \text{ Wm}^{-2}\text{K}^{-1}$. However, HTC between part and mold is considered variable with respect to temperature. The following table shows the HTC curve used for this test (Laschet, Jakumeit, and Benke, n.d.).

Temperature (K)	HTC ($\text{Wm}^{-2}\text{K}^{-1}$)
473.15	180.00
673.15	180.00
723.15	250.00
815.15	300.00
823.41	314.54
827.83	815.64
832.24	870.38
857.47	887.76
869.36	884.92
886.15	898.00
973.15	898.00

The remaining material properties follow the curves describe in the figures and tables below.

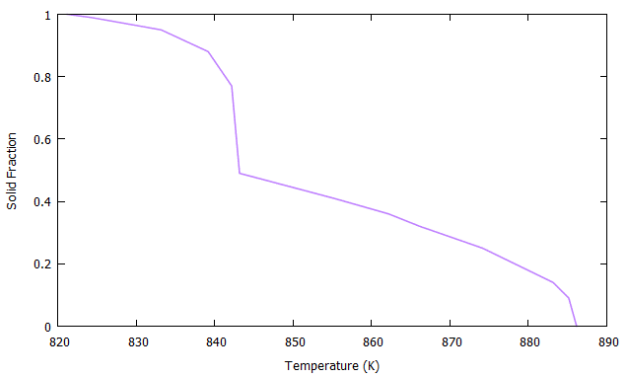


Temperature (K)	Thermal Conductivity (W/m K)
293.14	154.20
293.15	154.20
373.15	156.60
473.15	163.50
573.15	170.90
673.15	172.10
773.15	174.50
824.15	168.18
833.15	147.73
839.15	134.09
842.15	127.27
843.15	125.00
850.15	117.67
855.15	112.44
862.15	105.12
866.15	100.93
874.15	92.58
883.15	83.14
885.15	81.05
1173.15	80.00
1173.16	80.00



Temperature (K)	Specific heat (J/kg K)
293.14	919.00
293.15	919.00
373.15	940.00
473.15	965.00
573.15	991.00
673.15	1020.00
773.15	1045.00
821.15	1045.00
886.15	1045.00
1023.15	1045.00
1173.15	1045.00
1173.16	1045.00

Temperature (K)	Density (kg/m ³)
273.14	2675.00
273.15	2675.00
293.15	2675.00
373.15	2661.00
473.15	2642.00
573.15	2621.00
673.15	2599.00
773.15	2576.00
821.15	2565.00
886.15	2481.20
1023.15	2445.00
1173.15	2405.40
1173.16	2405.40



Temperature (K)	Solid Fraction
821.15	1.00
821.15	1.00
824.15	0.99
833.15	0.95
839.15	0.88
842.15	0.77
843.15	0.49
855.15	0.41
862.15	0.36
866.15	0.32
874.15	0.25
883.15	0.14
885.15	0.09
886.15	0.00
886.15	0.00

The mold is made from a low alloy steel with composition 0.14%C, 0.35%Si and 1.2%Mn. The initial temperature of the mold is 403.15K.

Mold Properties	
Density	7800 kg/m ³
Specific Heat	544 J/(kg K)
Conductivity	45.29 W/(m K)

The core is a quartz tube filled with oil bound sand, but it is modelled using exclusively sand properties. It has initial temperature 403.15K.

Core Properties	
Density	1500 kg/m ³
Specific Heat	800 J/(kg K)
Conductivity	0.9 W/(m K)

The insulation component covers the region above and below the whole set. Therefore, it is in direct contact with mold, part and core. The heat transfer coefficient with all components is fixed at $HTC_{All-Insulation}=400 \text{ Wm}^{-2}\text{K}^{-1}$. To simulate the insulation, both parts are designated as sleeves with the properties above described, very low conductivity and with constant density.

Insulation Properties	
Density	1000 kg/m ³
Specific Heat	1760 J/(kg K)
Conductivity	0.1 W/(m K)

MESH

To obtain accurate results when collecting the data from the different points of interest it is crucial to do a right meshing of the model.

In this case, as the measurements are obtained from the different components the mesh must be fine and homogeneous. Table 5 shows the element size for each component in the simulation. This configuration creates a grid with, at least, 250 000 elements in the liquid part. Low conductivities in components as the sleeves creates steep temperature gradients that require a fine mesh to capture results with accuracy.

The mesh details provided in this document correspond to the upper limit to element size in order to ensure good results. Coarser mesh does not improve considerably processing time and result in inaccuracies.

Component	Size
Cast Part	3.0 mm
Mold	3.0 mm
Core	3.0 mm

Results

The data is collected in certain points according to the experimental description of *Kron et al. [1]*. Considering the mid-height region (50mm) the temperature curve is measured at five different radii as shown in the following table.

Component	Radius
Core	8 mm
Cast Part	45 mm
	69 mm
Mold	77 mm

We proceed to compare the results of the *AMS solver* simulation to the data available in the literature of reference for each component. This includes a comparison between *Casts-Spand3D*, *MagmaSoft*, *Procast*, *Theracast* and experimental tests.

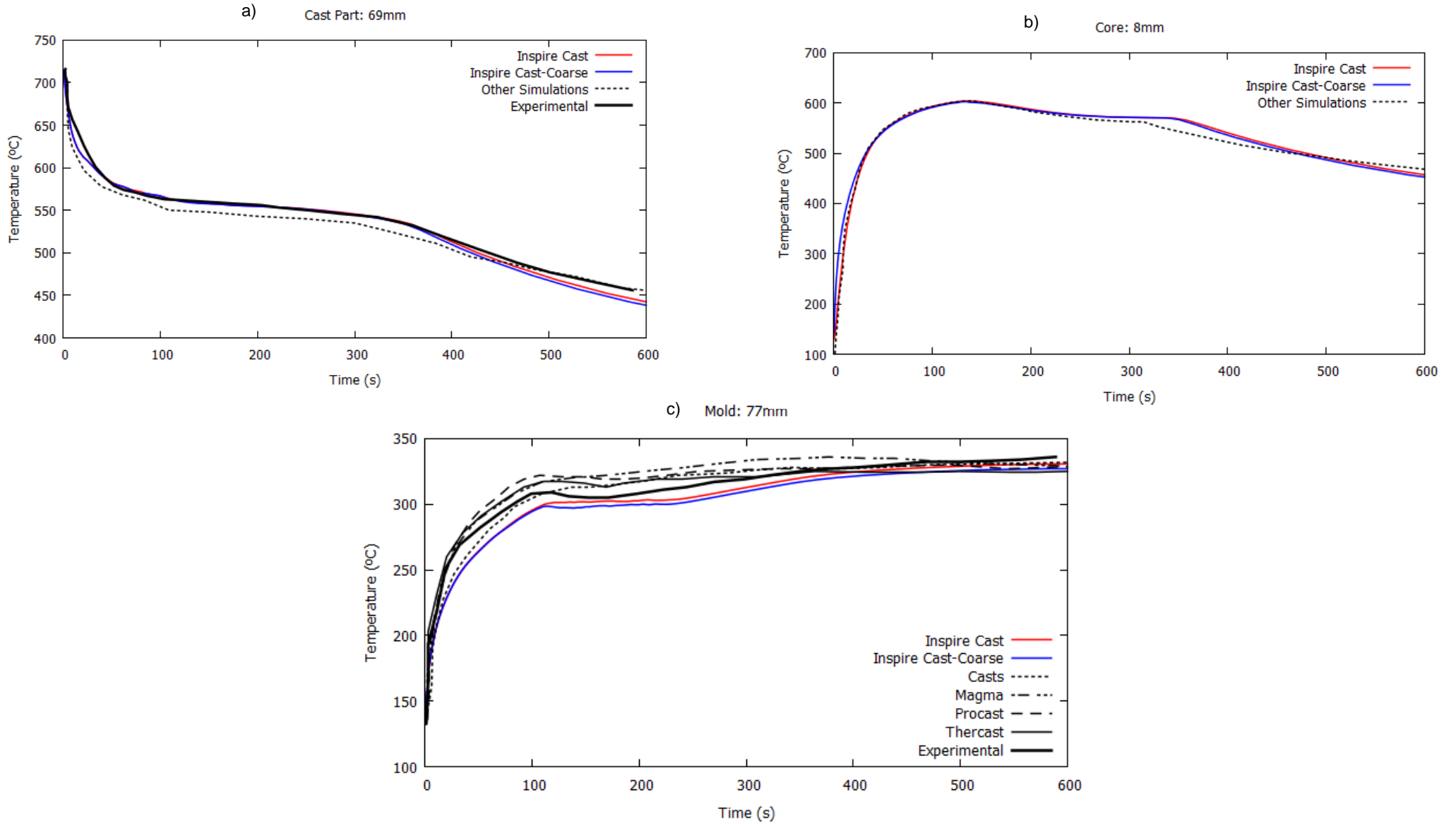
In Figure 8 is shown that the results obtained with the different simulation solvers are very similar to each other.

COARSE MESH

In this section, a coarser mesh is considered to run the same experiment. The new mesh has an element size of 6 mm, this corresponds to the double of the size of the previous test (see Figure 9). As shown in Figure 10, the results obtained when enlarging element size are very similar.

An increase of element size normally leads to accuracy loss but in this case this effect has not a great incidence on the results that remain good in relation to the reported in the reference work and temperature measurements do not deviate further than 5°C.

Figure 8. Results for A356 alloy casting simulation with variable heat transfer coefficient.



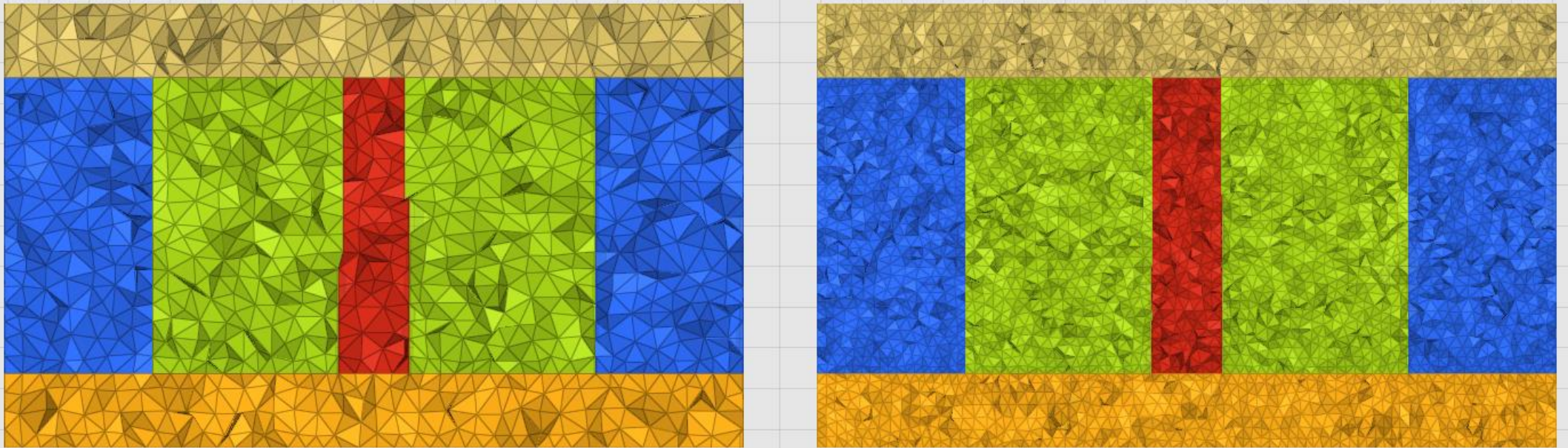


Figure 9. Mesh details: left) coarse mesh ; right) fine mesh.

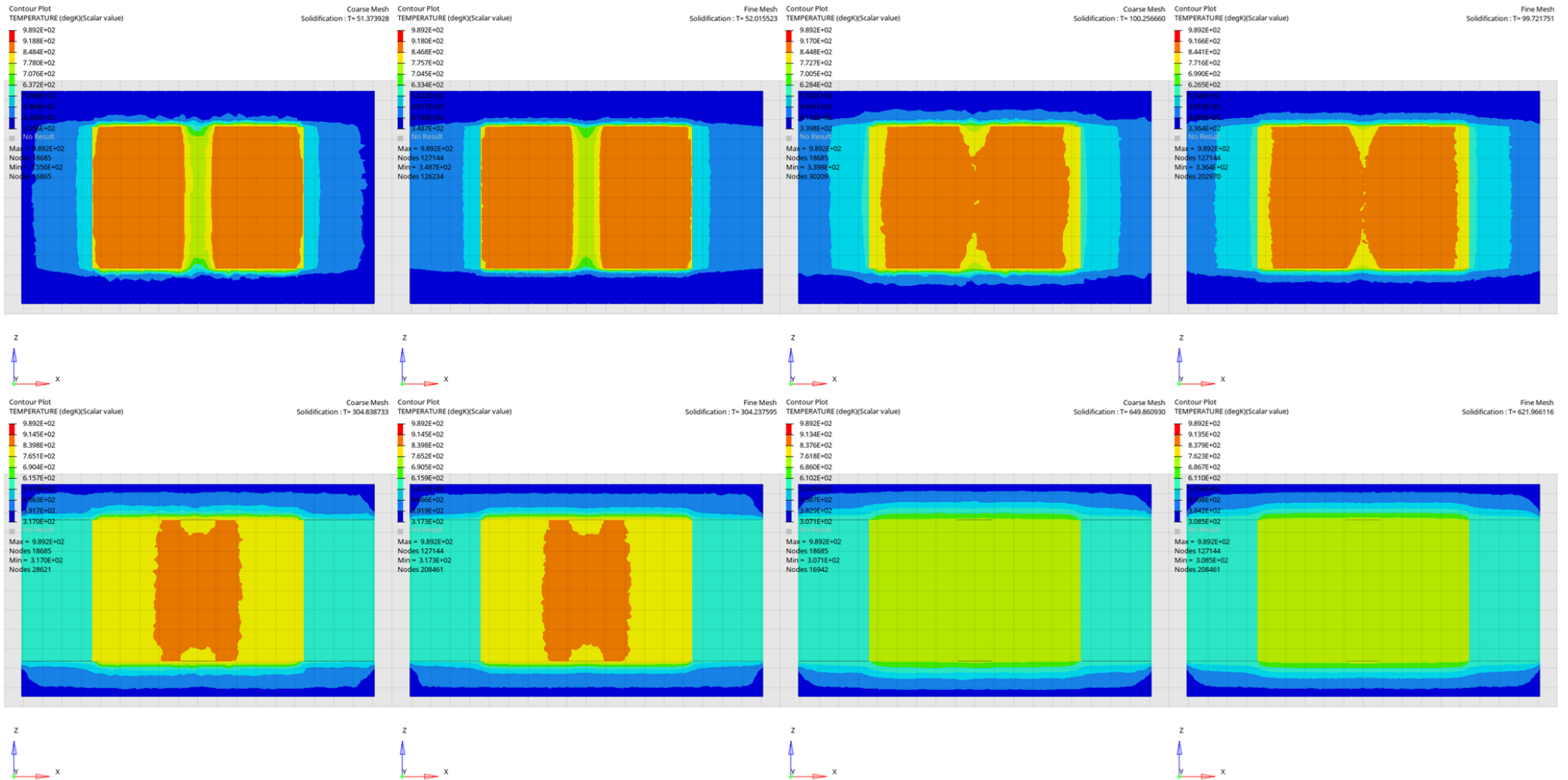


Figure 10. Temperature evolution during solidification (left - coarse mesh ; right - fine mesh) .

2. Prediction of Shrinkage Pore Volume Fraction Using the Niyama Criterion: WCB Steel Alloy

Objectives

The Niyama criteria allows to predict the amount of shrinkage porosity that forms during the solidification of metal alloy casting by considering temperature gradients along this process. This test aims to accurately define the Niyama contour plots in the casting simulations as this is one of the most used features.

Method and Description

The Niyama values are a classical term widely used in foundry industries. By accurately predicting Niyama values, it is possible to predict micro porosity as well. To replicate the experiment carried out by *Carlson et al.* (Carlson and Beckermann 2009) we consider the geometry shown in Figure 11, which involves a cylindrical riser, a squared plate and a mold.

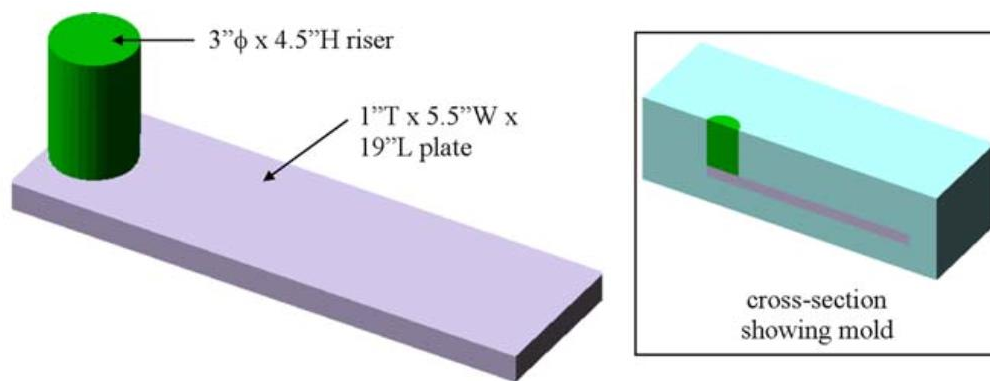


Figure 11. Geometry of the Set-up for the Niyama test (Carlson and Beckermann 2009).

The height of the riser is 114.3mm with a diameter of 76.2mm and the size of the plate is 25.4x140x483mm. The whole part is inside a mold of 680x360x360mm at 75.5mm of the right edge.

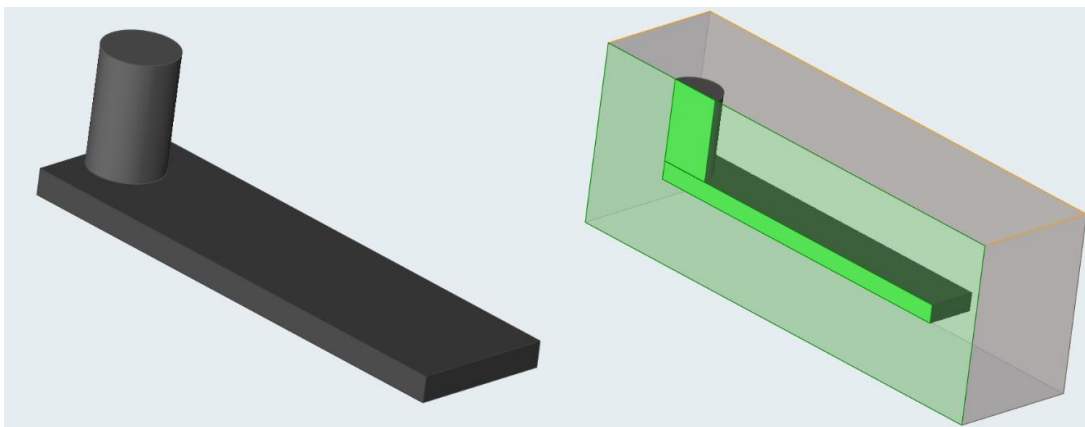


Figure 12. Geometry of the Inspire Cast simulation for the Niyama test.

Parameters

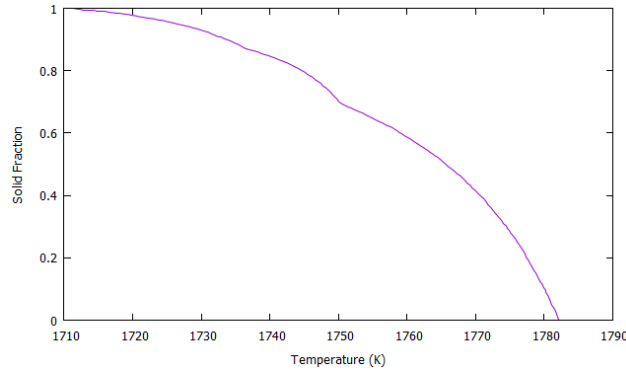
MATERIAL DETAILS

For each component, the material details are described in this section.

The alloy chosen for the cast part is an WCB steel with composition 0.19%C, 0.2%Cr, 1.25%Mn, 0.04%P, 0.045%S and 0.4%Si with an estimated initial temperature after filling of 1842.15K. The latent heat of this alloy is 230 kJ/kg.

HTC between part and mold is constant with value $HTC_{\text{Part-Mold}}=1000 \text{ Wm}^{-2}\text{K}^{-1}$. The dynamic viscosity is considered constant at a value of 0.0056 kg/(m s).

The rest of the properties are the default characteristics given by the data base of Inspire Cast (for Carbon Steel A126-WCB) except from the solid fraction that follows the curve shown below.



Temperature (K)	Solid Fraction	Temperature (K)	Solid Fraction
1711.35	1.000000	1724.46	0.960773
1711.97	0.997473	1725.35	0.955726
1712.87	0.994942	1726.33	0.950677
1713.31	0.994934	1732.93	0.907793
1714.03	0.992405	1733.82	0.898972
1714.38	0.992399	1734.27	0.895190
1715.18	0.991127	1738.28	0.859899
1715.63	0.991119	1738.72	0.854860
1717.06	0.986062	1740.15	0.844771
1717.50	0.984796	1744.16	0.806964
1718.04	0.984787	1744.52	0.801926
1718.57	0.982262	1747.02	0.765404
1719.46	0.979730	1747.73	0.750297
1719.91	0.977206	1749.96	0.703717
1720.80	0.973417	1753.97	0.658362
1721.25	0.972151	1761.64	0.563886
1721.87	0.969624	1762.09	0.557589
1722.76	0.967093	1765.39	0.504700
1723.21	0.965827	1765.74	0.498405
1723.57	0.963305	1768.06	0.456854
1724.01	0.962039	1770.47	0.403981

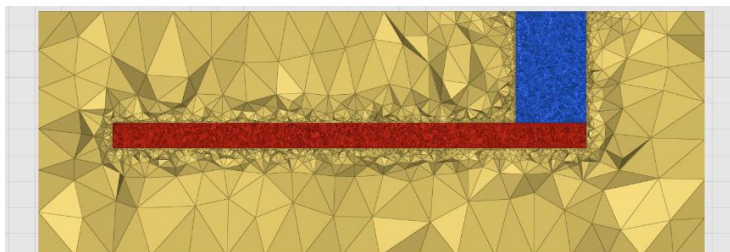
The mold is made from a FURAN sand, whose initial temperature is considered as 293.15K.

The properties of the material correspond to the default properties in the Inspire Cast Data Base.

Component	Material	Initial Temperature (K)
Cast Part	WCB Steel	1842.15
Mold	FURAN Sand	293.15

MESH

In the table below the size of the elements for the different components is detailed. The finer the mesh, the more accurate the results when considering the central region where the most part of the microporosity occurs as it is shown in the 'Results' section.



Component	Size
Cast Part	3.0 mm
Mold	10.0 mm
Riser	3.0 mm

Results

Through the information available in the literature it is possible to compare the results of this simulation to experimental tests and another simulation software (*MagmaSoft*). We proceed to compare the porosity and microporosity percentage and niyama values in the mid-plate region (height of 12.7mm).

In the Figure 13 and Figure 14 the results of porosity and microporosity percentage obtained for the experimental tests are shown in comparison to the AMS solver Simulation results. The porosity prediction of the simulation is within the average porosity obtained in the 15 experimental plates showing greater impact of porosity (red and yellow points) in the same zones. The range of scatter given by *AMS solver* is very close to the presented by *Carlson et al.* (Carlson and Beckermann 2009) experiments.

As for the niyama prediction shown in Figure 15, the results present the similar behavior in both cases. The central region shows a higher porosity rate (lower niyama values), which decreases as it approaches the edges. Overall, we conclude that the maximum porosity is present in the central region reaching and decreasing to zero as it approaches the edges.

COARSE MESH

Niyama values and microporosity results are parameters that depend highly on element size. Therefore, in general we always expect to obtain more accurate results when considering a finer mesh.

Figure 16 shows the comparison between niyama values for a mesh of elements with size 5mm (above) and a 2mm element size (below). Due to the increase in size the contour is less homogeneous, but the global prediction follows the same lines as the original results. This behavior with mesh size is maintained also when comparing microporosity results (Figure 17) in which homogeneity in the contour is decreased and accuracy is hindered so that the top values obtained for a fine mesh are not reached.

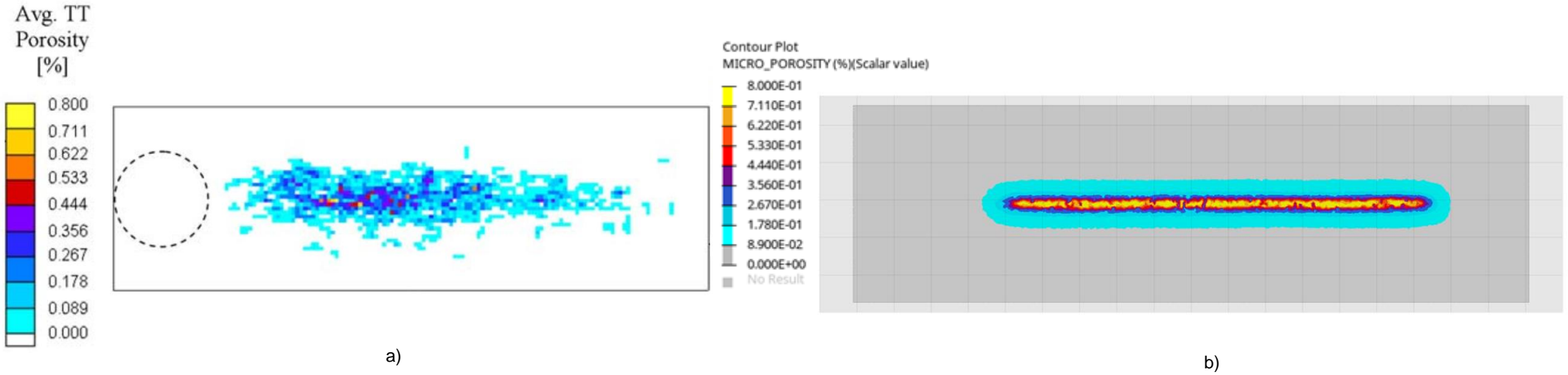


Figure 13. Micro Porosity comparison between a) Experimental test (average of 15 plates) (Carlson and Beckermann 2009); b) AMS solver Simulation.

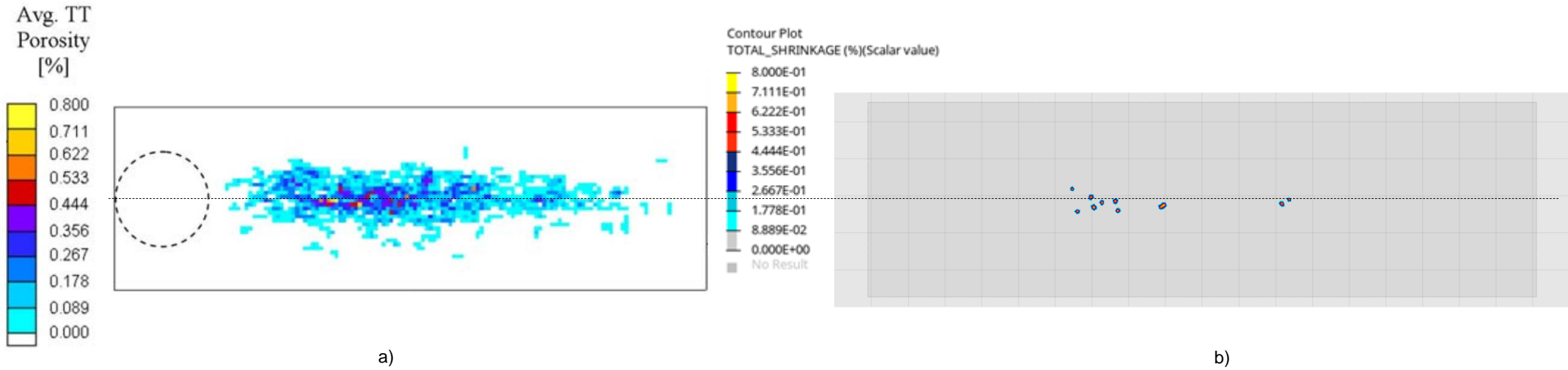


Figure 14. Porosity comparison between a) Experimental test (average of 15 plates) (Carlson and Beckermann 2009); b) AMS

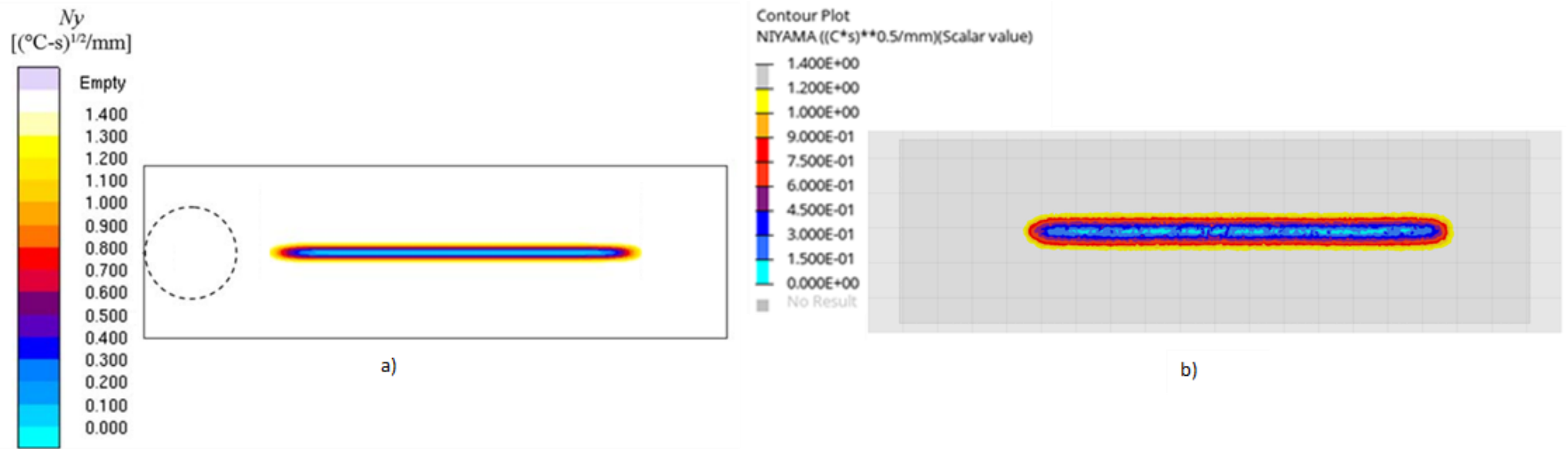


Figure 15. Niyama comparison between a) Predicted Niyama Distribution (MagmaSoft) (Carlson and Beckermann 2009); b) AMS solver Simulation.

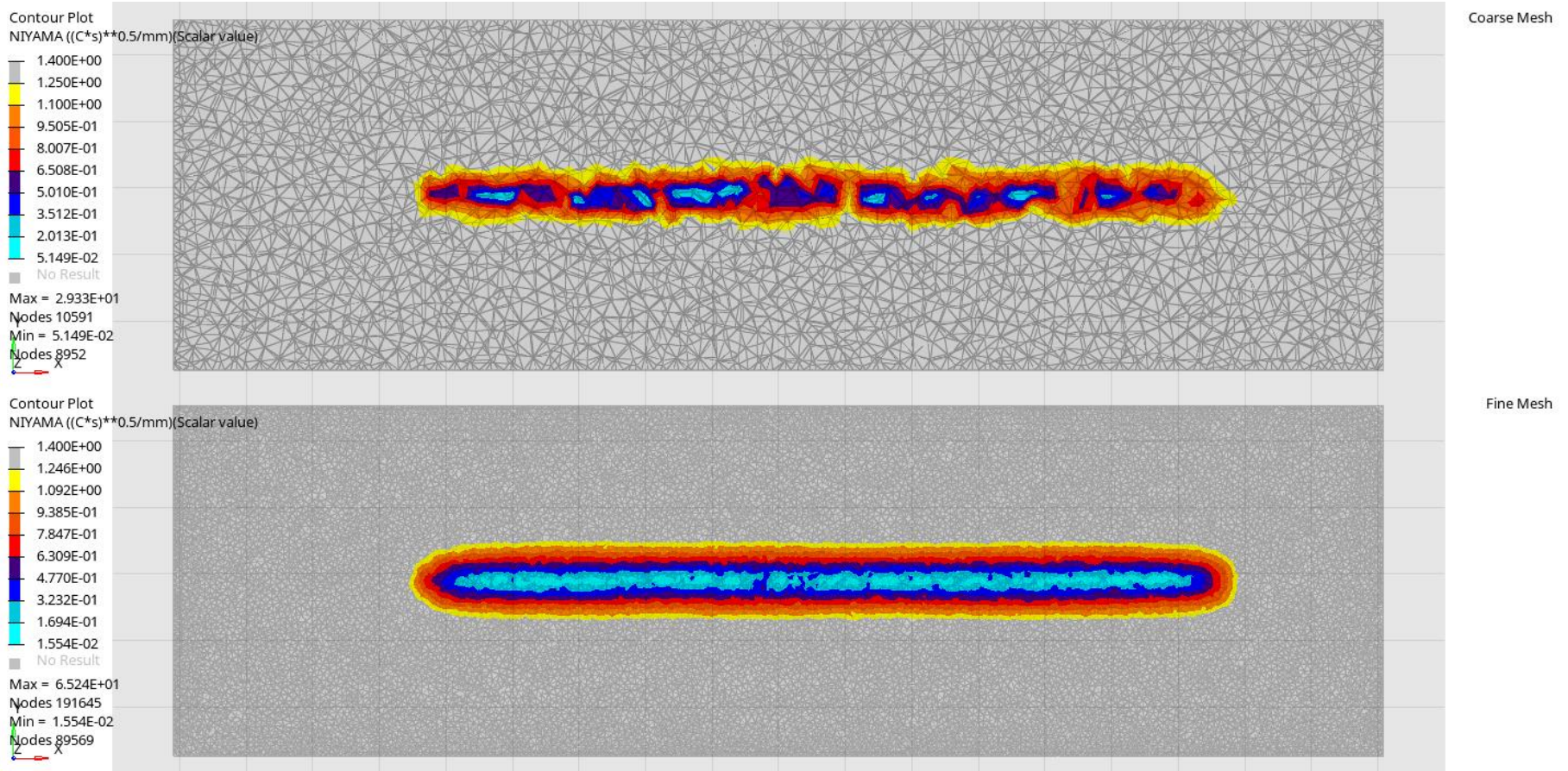


Figure 16. Niyama values for different mesh sizes.

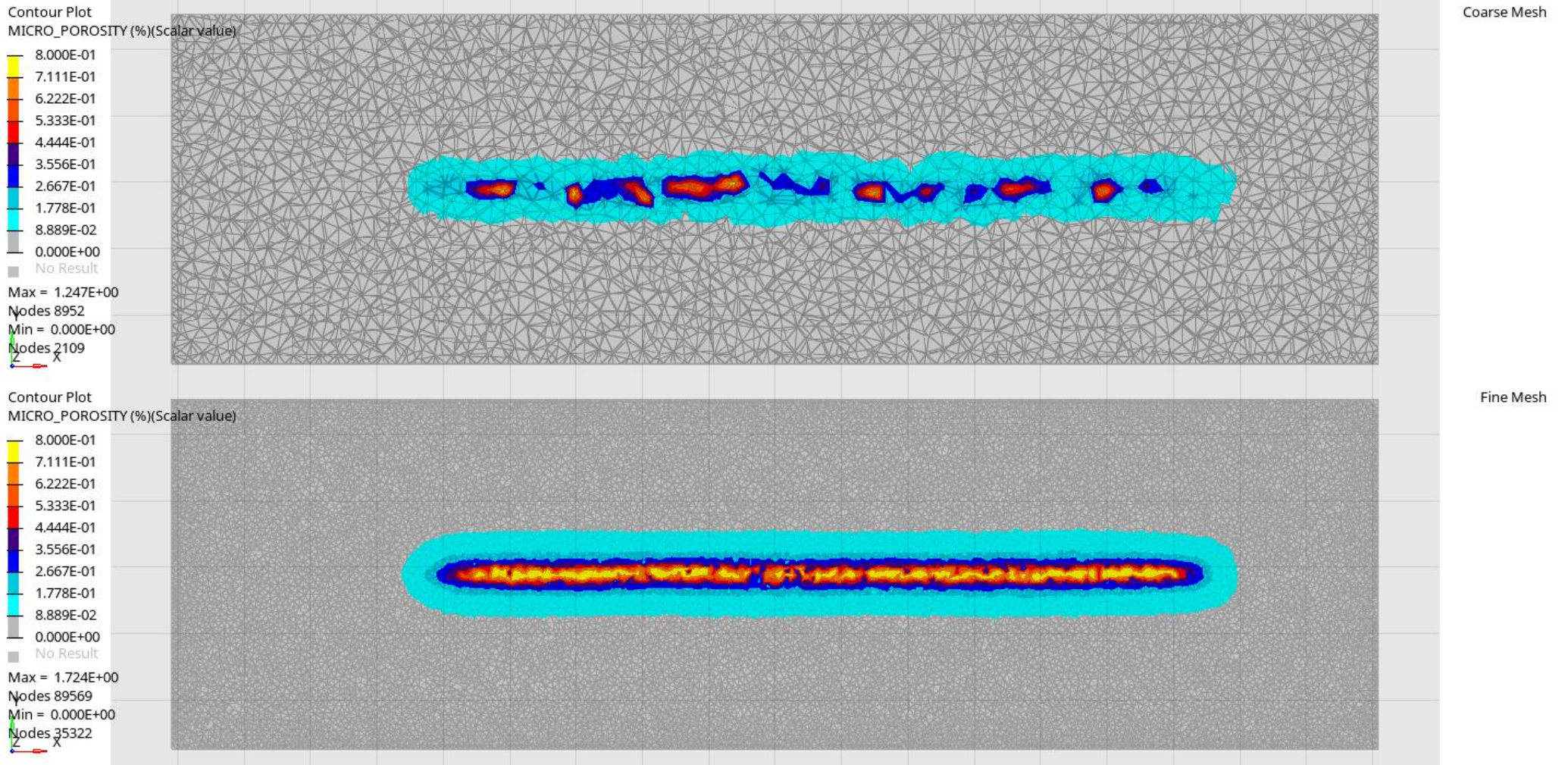


Figure 17. Microporosity results for different sizes

3. Validation Tests for Shrinkage Defects Prediction in Cast Iron Samples

Objectives

This test aims to analyze the shrinkage defect phenomena occurring in cast iron castings by inspecting pipe shrinkage formation during solidification. The distribution and creation of porosity defects is the result of the balance between liquid and solid fraction in the solidifying zones where shrinkage occurs. The validation of these defects with experimental results is crucial to ensure good results and performance of casting parts. Although porosity in general is unavoidable, its control and minimization are the main challenges that the foundry engineers face, always increased by complexity of the part geometry.

Method and Description

This test is designed to study shrinkage formation. The geometry required for this test is based on the reference 'Polish Branch Standard BN-80/4051-11' with slight modifications which allows to prevent the start of crystallization before de mold is filled due to presence of heat nodes. This is an interesting feature for the purpose of controlling and shaping the solidification front. In this case it allows to form a compacted shrinkage cavity connected to the ambient with the support of the several heat nodes and massive chill. The accurate geometry used by Hajkowski (Hajkowski et al. 2017) is shown in Figure 18.

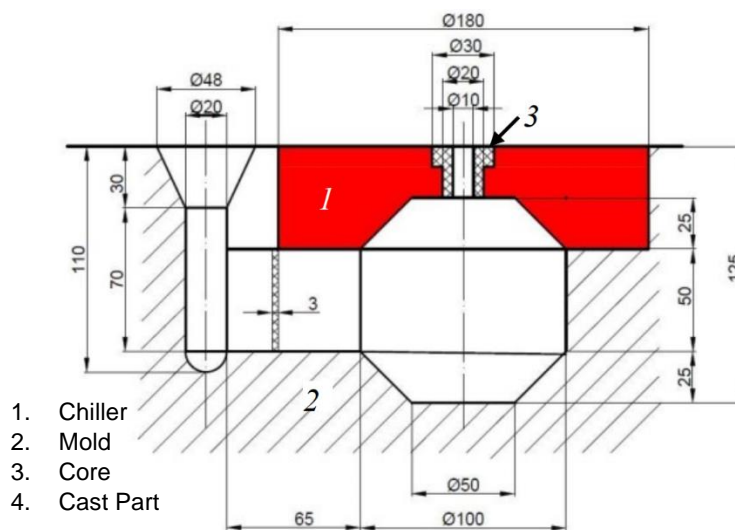


Figure 18. Geometry of the Set-up for the porosity test (Hajkowski et al. 2017).

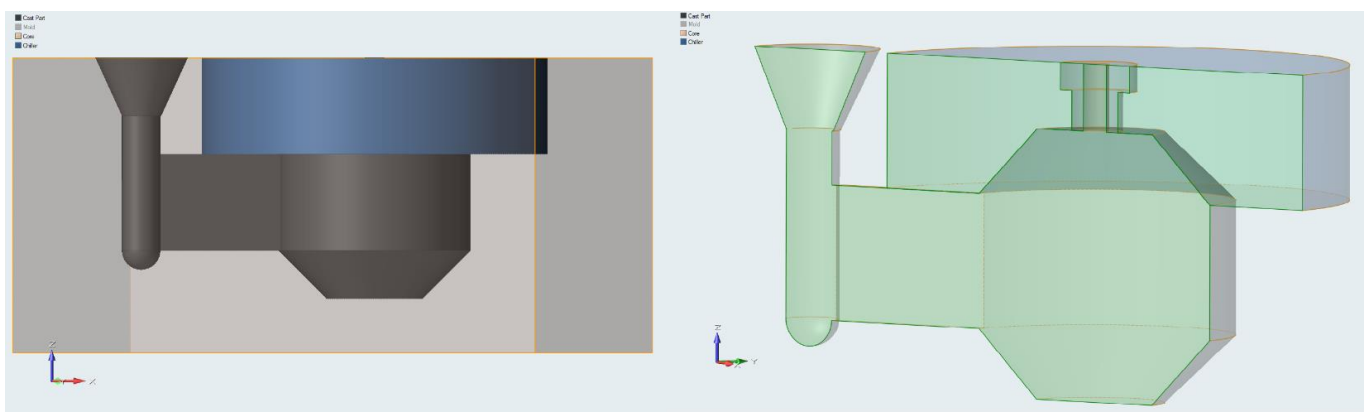


Figure 19. Geometry of the Inspire Cast simulation for the porosity test.

Parameters

MATERIAL DETAILS

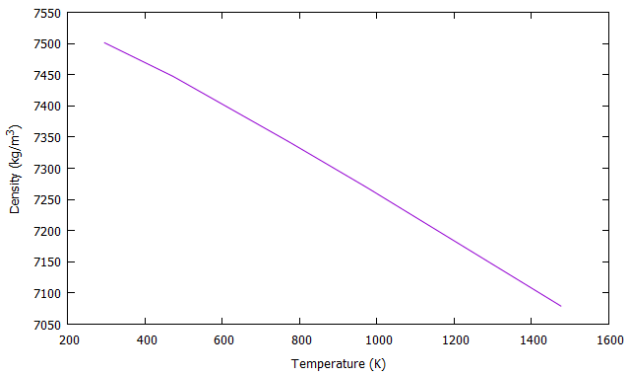
For each component, the material details are described in this section.

The alloy chosen for the cast part is a Cast Iron with designation GJS-600-3 available in the data base of Inspire Cast with an estimated initial temperature after filling of 1633.15K. The **latent heat of this alloy is 251.8 kJ/kg**.

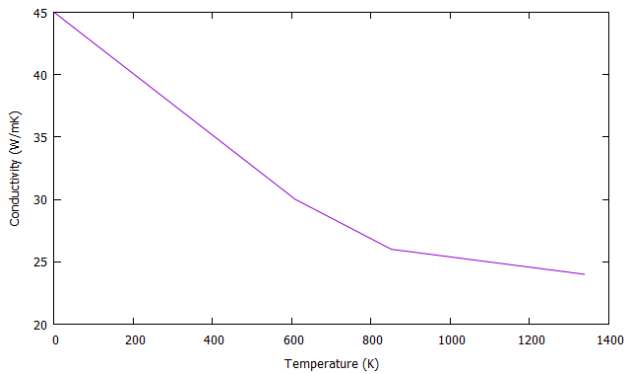
The **shrinkage factor** in this case, although is not detailed explicitly in the literature, has been considered as a **2.5%**, very common for cast irons. HTC between part and chiller is constant with value $HTC_{Part-Chiller}=400 \text{ Wm}^{-2}\text{K}^{-1}$. The porosity criteria are set by default, considering the **critical cut off value for porosity as 0.7**.

The mold is made from a Green sand, whose initial temperature is considered as 313.15K. The core is made from a Silica sand, whose initial temperature is considered as 313.15K. All the material details of the mold and core, and the remaining for the cast part are the default properties from the Inspire Cast Data Base.

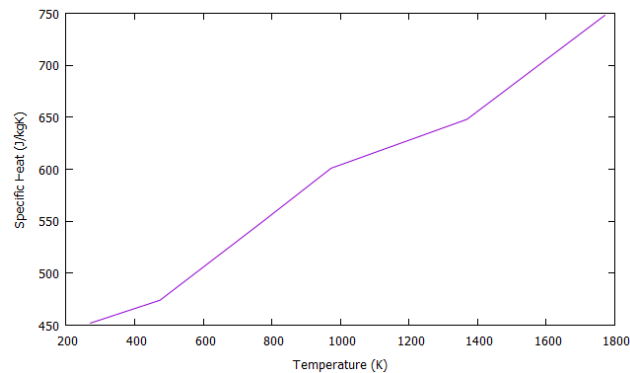
The chiller is made from steel, whose initial temperature is considered as 313.15K. The following figures and tables show the curves used for the different material properties.



Temperature (K)	Density (kg/m3)
293.14	7501.31
295.57	7501.31
473.79	7447.11
773.01	7342.38
974.00	7269.81
1476.42	7079.65
1476.43	7079.65



Temperature (K)	Conductivity (W/m K)
293.14	45.01
293.15	45.01
609.2	30.61
851.15	26.23
1338.15	24.06
1338.16	24.06

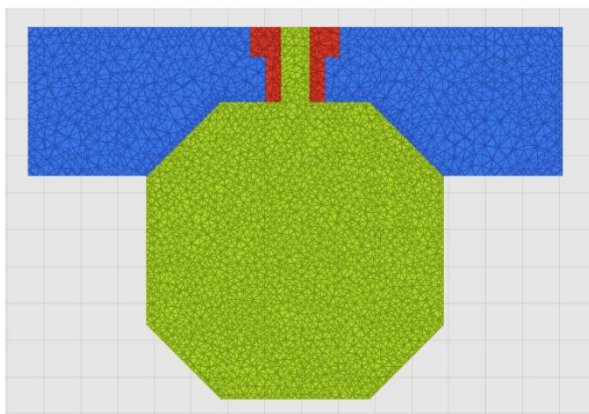


Temperature (K)	Specific Heat (J/kg K)
271.85	452.00
271.86	452.00
474.07	474.56
771.61	549.18
973.75	601.15
1369.09	648.94
1771.11	748.88
1771.12	748.88

Component	Material	Initial Temperature (K)
Cast Part	GJS-600-3	1633.15
Mold	Green Sand	313.15
Chiller	Steel	313.15
Core	Silica Sand	313.15

MESH

In the table below the element size for the different components is detailed. When considering porosity and shrinkage results, meshing correctly makes a great difference in the accuracy of the results. Meshing the mold with a very fine mesh, on the contrary, may extend processing time without any contribution. The reference work refers to a mesh of element size of 2mm.



Component	Size
Cast Part	2.0 mm
Mold	15.0 mm
Chiller	3.0 mm
Core	2.6 mm

Results

Through the information available in the literature it is possible to compare the results of the *AMS solver* simulation to experimental tests. We proceed to analyze the porosity shrinkage results.

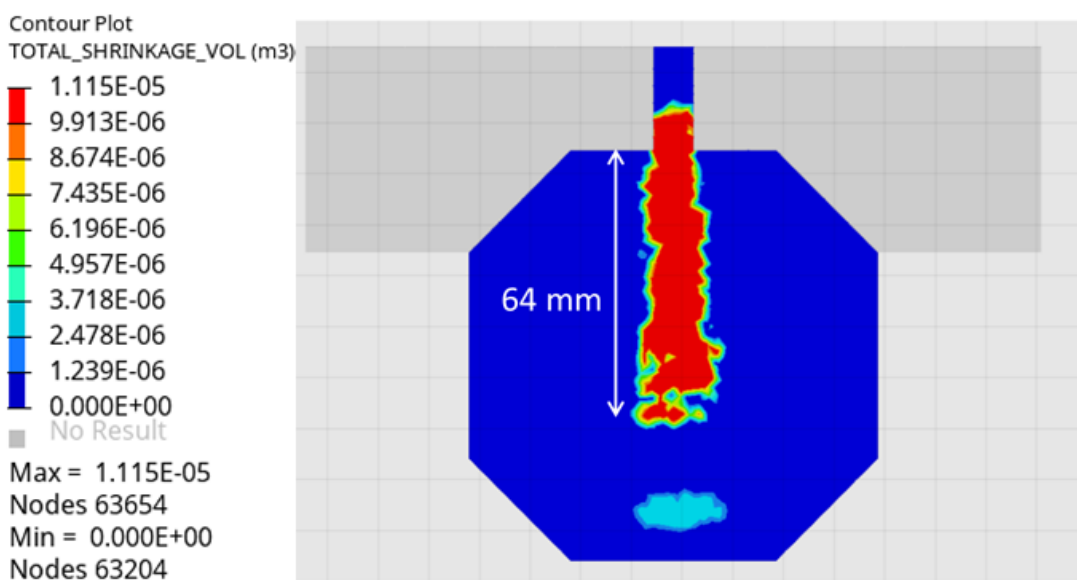


Figure 20. Shrinkage simulation results using the AMS solver.

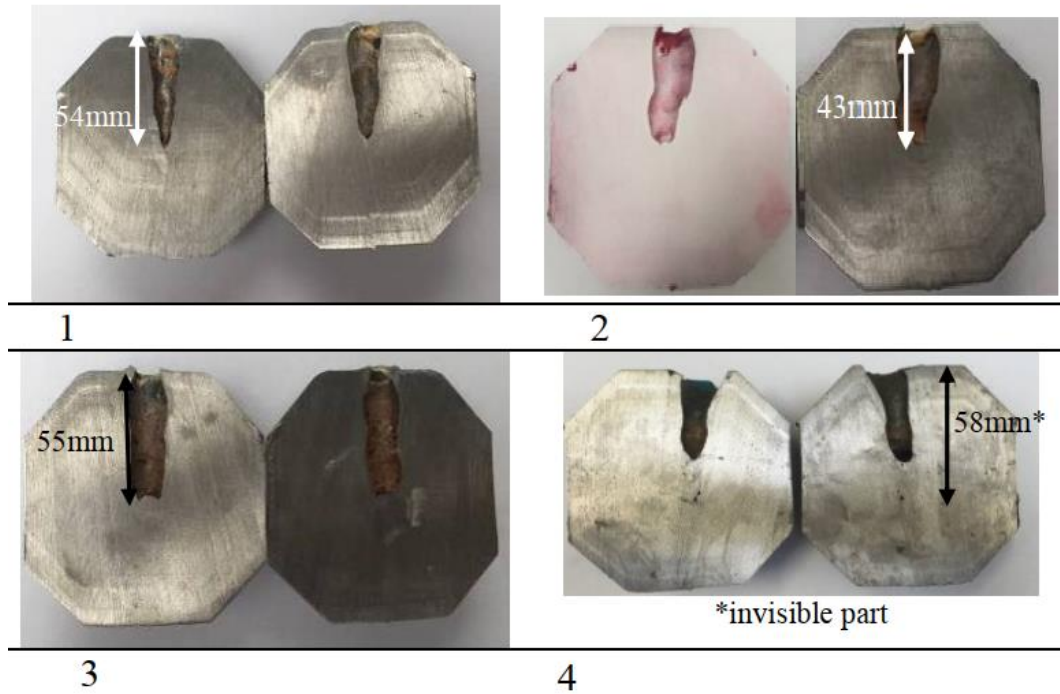


Figure 21. Shrinkage results reported in the reference work (Hajkowski et al. 2017).

Figure 20 and Figure 21 show the results obtained in the *AMS solver* simulation and the reference literature (Hajkowski et al. 2017), respectively. The central region presents a higher shrinkage effect than the rest of the part, which is due to the chiller’s effect on the solidification front. When comparing to experimental results, we see that *AMS solver* predicts shrinkage very accurately in both regions where it appears, where one shows greater incidence (upper) than the other (lower) as it is the zone in contact with the ambient. The ability to determine the small porosity located in the lower region indicates a high level of accuracy.

Finally, the table below shows the numerical results presented in the reference work in comparison to the obtained by the simulation. These correspond to a deviation of less than the 20%, considering that the experimental deviation of the results shown in the literature reaches the 20%, the results lie within the acceptable range.

Test	Porosity (cm ³)	Porosity (%)	Defect Range
Experimental - 1	7.9	1.13	54
Experimental - 2	8.2	1.17	43
Experimental - 3	8.9	1.27	55
Experimental	9.1	1.3	58
AMS solver	11.0	1.7	64

COARSE MESH

Porosity results are very mesh dependent, therefore, the finer the mesh the more accurate the result. Nonetheless, as shown in Figure 22, in this case results are very similar when changing element size in the mesh although they show slight differences as expected and due to the nature of the calculation.

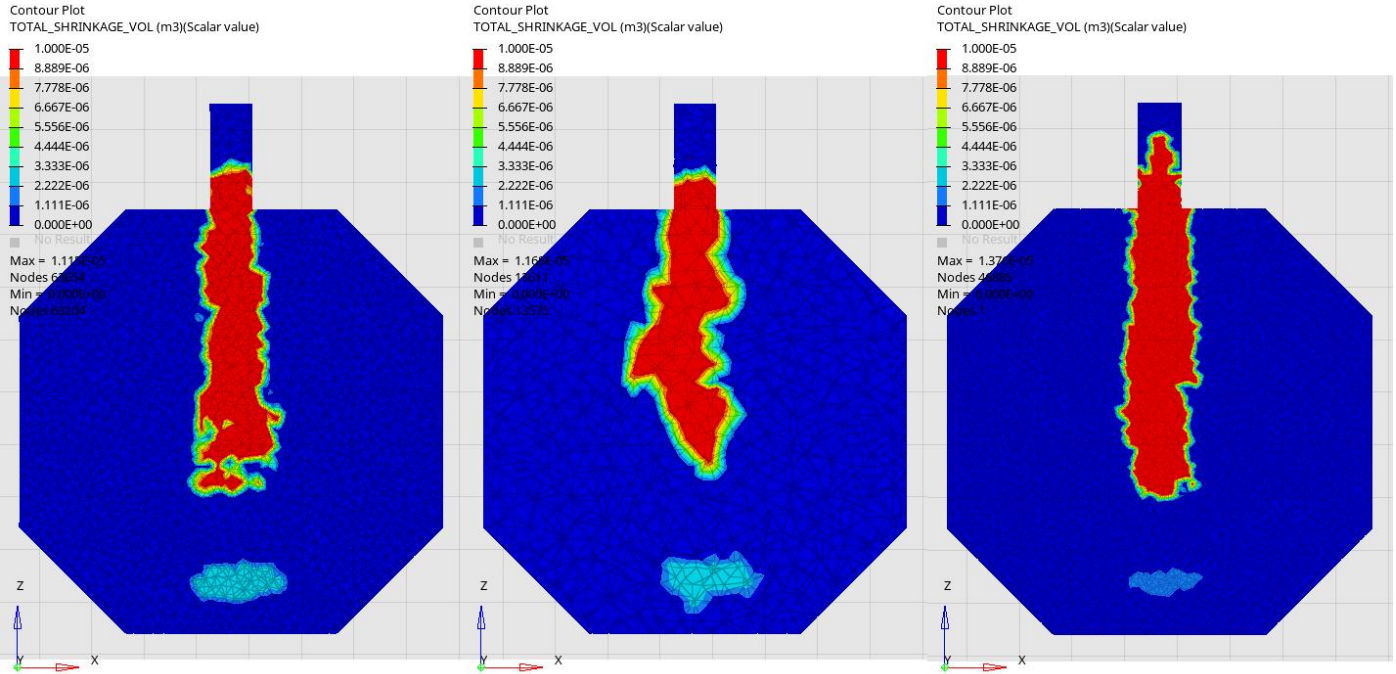


Figure 22. Results obtained for different element sizes : left) 2 mm; center) 5 mm; right) 1mm.

4. Thermal Cup Test

Objectives

This experiment is focused on capturing phenomenological aspects of the solidification process without referring to the phenomena occurring at the microscale level. Therefore, the main goal is to characterize the solidification process without considering further details but obtaining the most realistic temperature evolution. In this case, the model considered is referred to a thermal process already consolidated in the industrial practices and serves of great help in order to predict solidification phenomena by analyzing latent heat and heat release mechanisms using the solid fraction curve.

Method and Description

This test is based on the behavior analysis of a thermal cup, widely use in foundry with the purpose of analyzing and enhancing the capabilities of the solidification and predict the solid fraction as a function of temperature and requiring very easy calibration. This experiment allows testing temperature curves during solidification with very simple and standardized geometry (commercially known as Quick Cup). In order to replicate the results obtained by *M. Chiumenti et al.* (Chiumenti, Cervera, and Salsi 2018) the geometry of reference is shown in Figure 23.

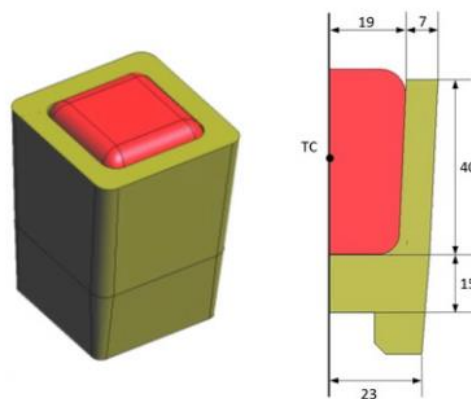


Figure 23. Geometry of the Set-up for the Thermal Cup Test (Chiumenti, Cervera, and Salsi 2018).

In Figure 24 we present the geometry developed using *Inspire Cast*.

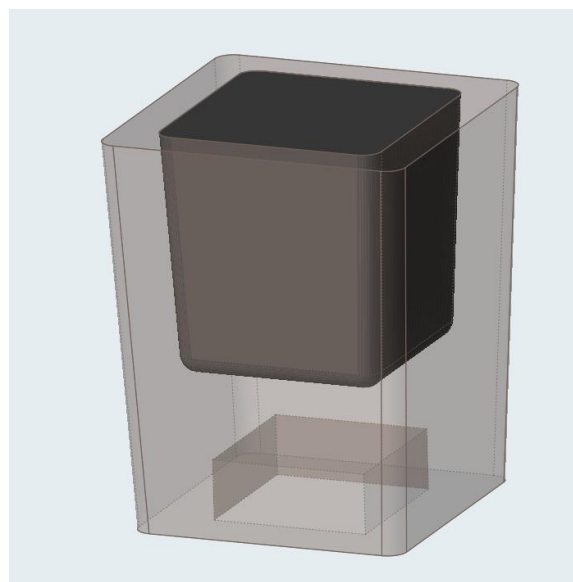


Figure 24. Geometry of the Inspire Cast Simulation for the Thermal Cup Test.

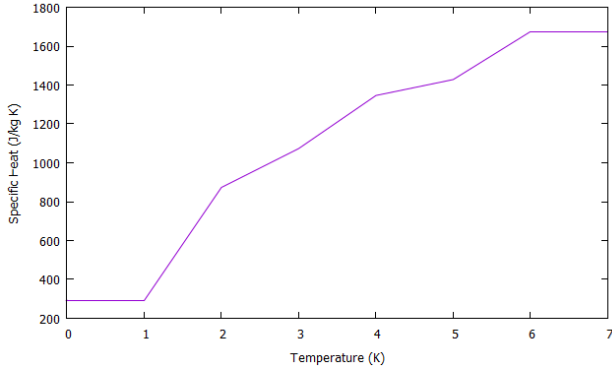
Parameters

MATERIAL DETAILS

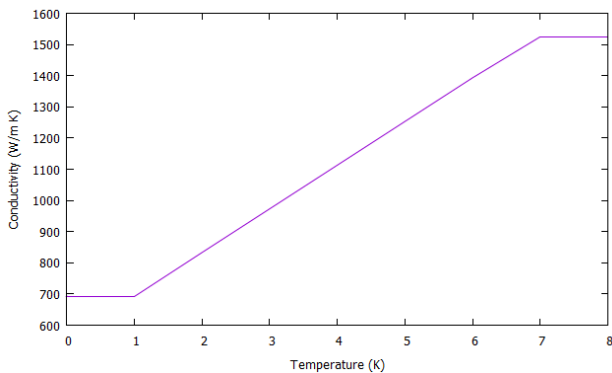
For each component, the material details are described in this section.

The cast part is a Cast Iron of composition 3.52%C, 2.18%Si, 0.29%Mn and 0.01%S with an estimated pouring temperature of 1573.15K. According to the authors, the **density corresponds to 7000 kg/m³** and the **latent heat to 228097 J/kg**. The heat transfer coefficient considered with the ambient is constant with value **HTC_{Part-Ambient}=50 Wm⁻²K⁻¹**.

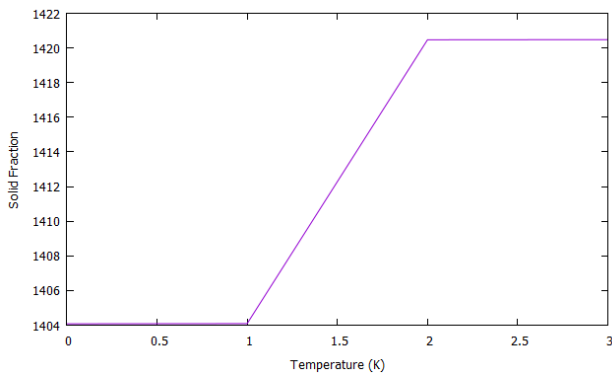
The remaining material properties of the casting are now described.



Temperature (K)	Specific Heat (J/kg K)
293.14	500.0
293.15	500.0
873.15	750.0
1073.15	750.0
1346.15	820.0
1428.15	240.0
1673.15	900.0
1673.16	900.0



Temperature (K)	Conductivity (W/m K)
693.14	41.0
693.15	41.0
833.15	37.0
973.15	33.6
1113.15	28.0
1253.15	22.5
1393.15	18.8
1523.15	65.0
1523.16	65.0



Temperature (K)	Solid Fraction
1404.08	1.0
1404.09	1.0
1420.47	0.0
1420.48	0.0

The mold part is a Resin Bonded Sand with an estimated initial temperature of 293.15K. The material properties are considered constant by the authors. Where the **density has a value of 1550 kg/m³**, **thermal conductivity of 0.8 W/mK** and **specific heat of 1000 J/kg K**.

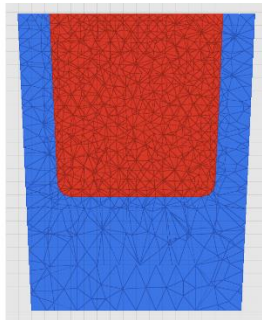
The heat transfer coefficient considered with the ambient is constant with value **HTC_{Part-Ambient}=50 Wm⁻²K⁻¹**. HTC between mold and part is also constant and corresponds to **HTC_{Part-Mold}=500 Wm⁻²K⁻¹**.

The properties of the material correspond to the default properties in the Inspire Cast Data Base.

Component	Material	Initial Temperature (K)
Cast Part	Aluminium A7075	1573.15
Mold	Resin Bonded Sand	293.15

MESH

In the table below the size of the mesh for the different components is detailed. In this case, we make sure to have at least two elements in the mold thickness. As for the casting, we consider the mesh slightly smaller as it is the region where the results are measured.



Component	Size
Cast Part	2.0 mm
Mold	(factor) 2.3

Results

It is now possible to compare the results of this simulation with *AMS solver* to experimental tests carried out by the reference literature. As shown in Figure 25, the temperature curve measured in the geometrical center of the casting follows the global experimental tendency along the whole solidification process.

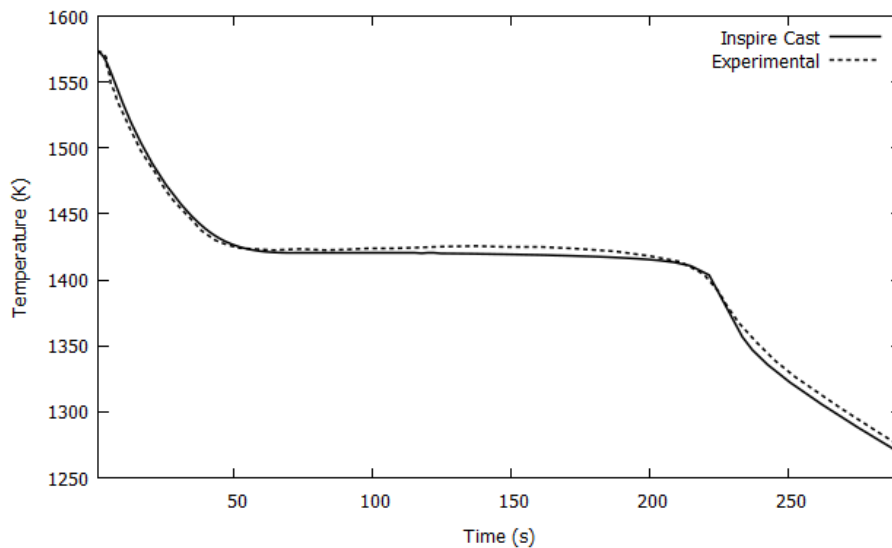


Figure 25. Results of the AMS Solver Simulation.

5. Tatur Test

Objectives

The tatur test technique is one of the most common methods to evaluate porosity in aluminum alloys. By replicating this experiment, we aim to validate porosity characterization, which is one of the major defects present in aluminum castings. To this purpose, results are compared to other software measurements and experimental tests, so that the shrinkage and porosity are accurately localized by the solidification process model.

Method and Description

This is a typical test used to analyze porosity formation in aluminum alloys. The experiment, as described by the literature (Chouchane et al. 2015) and (Haj, Bouayad, and Alami 2018), presents the geometry shown in Figure 26, composed by a permanent steel mold with standardized geometry.

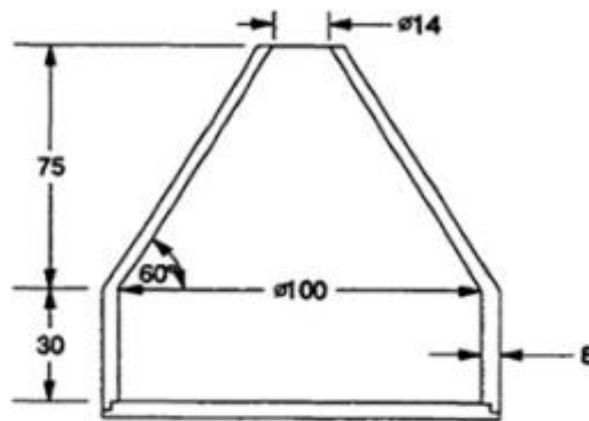


Figure 26. Geometry of the experimental Set-up for the Tatur Test (Brůna, Sládek, and Kucharčík 2012).

During the experiment, the melt is poured through the preheated mold orifice and allowed to solidify without any further melt addition. Due to contraction in absence of any riser and the conic design, the formation of porosity in the part is favored.

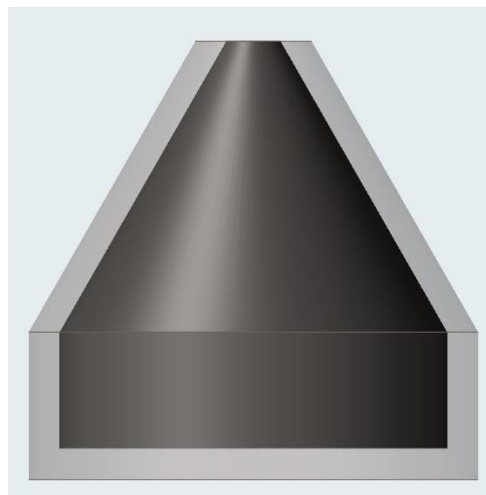


Figure 27. Geometry of the Inspire Cast simulation for the Tatur Test.

Parameters

MATERIAL DETAILS

For each component, the material details are described in this section.

The alloy chosen for the cast part is AlSi9 with an estimated initial temperature after filling of 989.15K. For the solid fraction, **liquidus temperature is considered 871.15K** and **solidus temperature 819.15K**, in this case, due to lack of information in the literature related to the solid fraction curve, it is considered linear.

The **shrinkage factor** in this case, although is not detailed explicitly in the literature, has been considered as a **5%**, very common for aluminum alloys.

The mold is made from a low alloy steel with denomination H13. The initial temperature of the mold is 423.15K.

Further material details are considered as the default properties from the Inspire Cast Data Base.

Component	Material	Initial Temperature (K)
Cast Part	AlSi9	973.15
Mold	H13	423.15

MESH

The following table shows the element sizes for each component in the simulation. Element size in the liquid part is very important in order to accurately determine porosity formation when this is expected to have low values. This way we ensure at least 100 000 elements in the model.

Component	Size
Cast Part	1.5 mm
Mold	3.0 mm

Results

We proceed to compare the results of the *AMS solver* simulation to the results available in the literature (Chouchane et al. 2015), where the same test was performed using a different software.

Figure 28 and Figure 29 show the comparison between the solid fraction evolution between the simulations with the different solvers. In general, we can confirm that the solidification follows the same tendency and at the same time. The solidification time reported by the literature is **161 seconds** for the other software simulation, which is also the case for the AMS result. The last region to solidify and the cause of the inner shrinkage is similarly located when comparing both cases. It is interesting to highlight that it seems that the beginning of the cooling happens slightly faster for the AMS simulation, which may be related to that HTC coefficients between parts that are not detailed in the reference work.

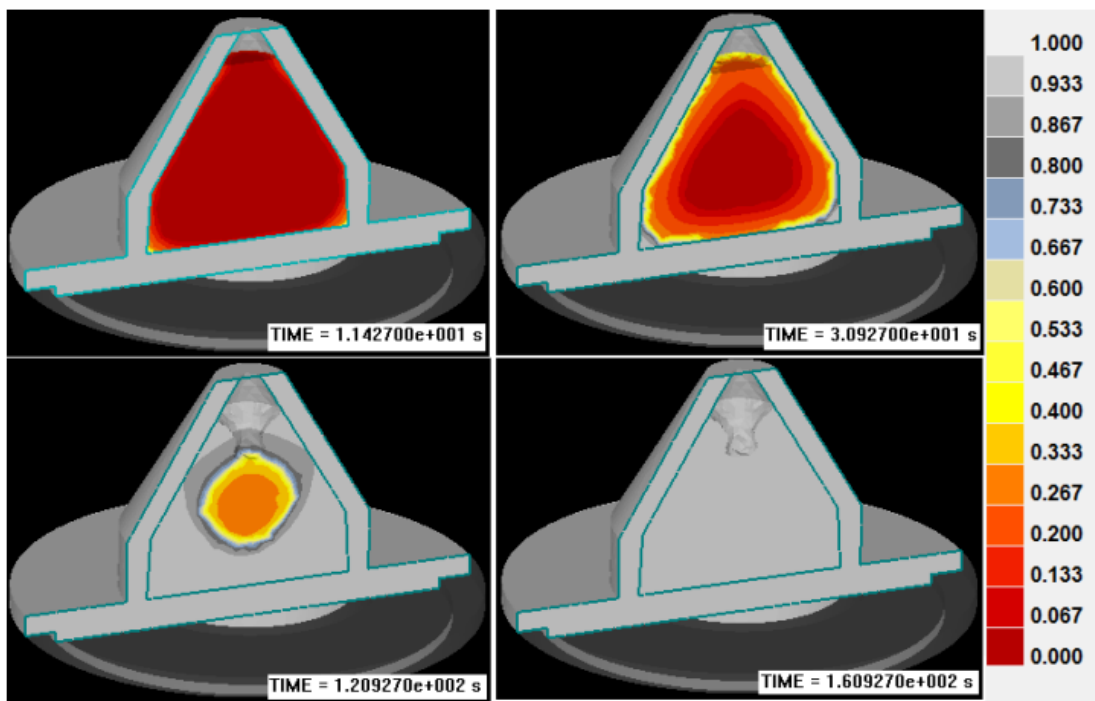


Figure 28. Procast solid fraction prediction (Hag, Baouayad, and Alami 2015).

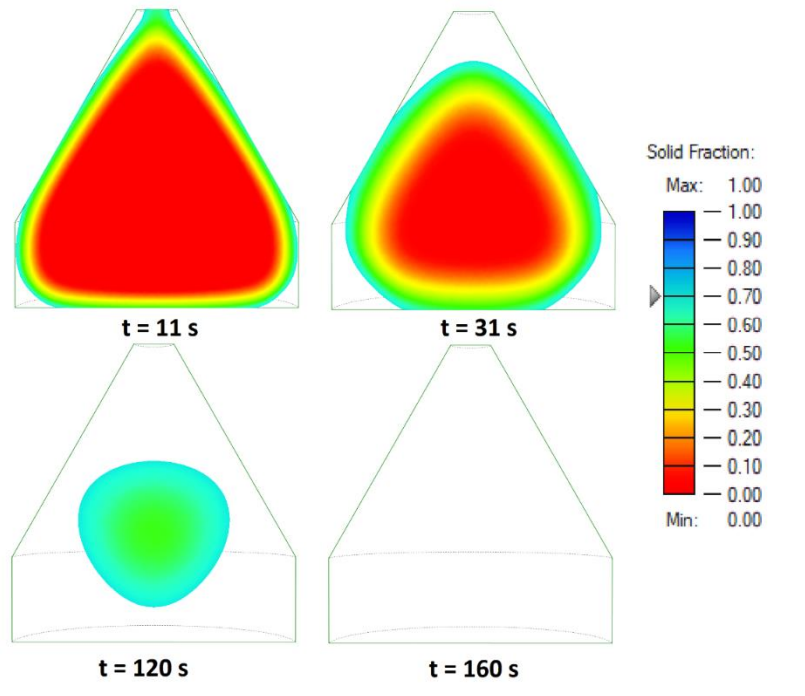


Figure 29. AMS Solver solid fraction prediction

The following results show the temperature evolution along solidification. We observe in Figure 30 and Figure 31, as expected from the solid fraction results, that the inner region of the cast presents the higher temperatures in the different time steps selected for this comparison. Meanwhile the outer region cools down faster due to its contact with the mold which presents a low initial temperature (150°C) in comparison to the 700°C the metal is poured at.

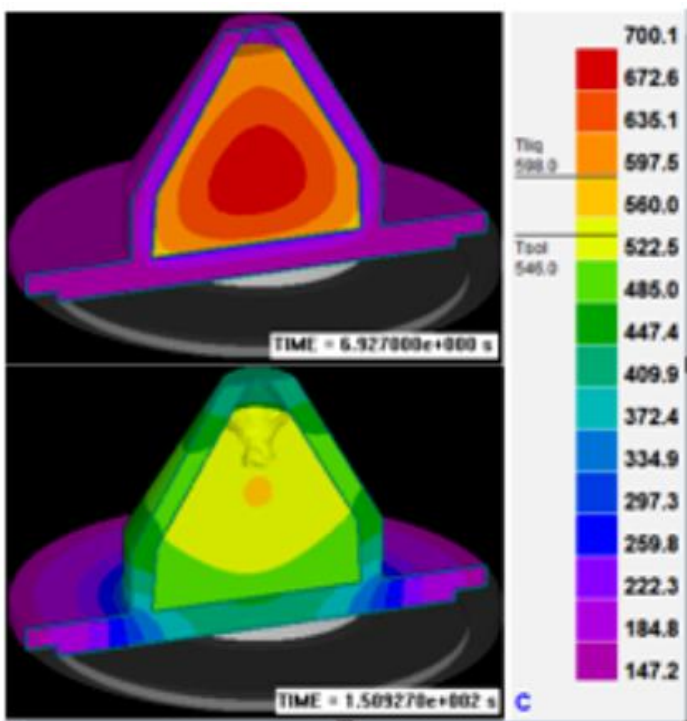


Figure 31. Temperature evolution in the Procast simulation (Hag, Baouayad, and Alami 2015)

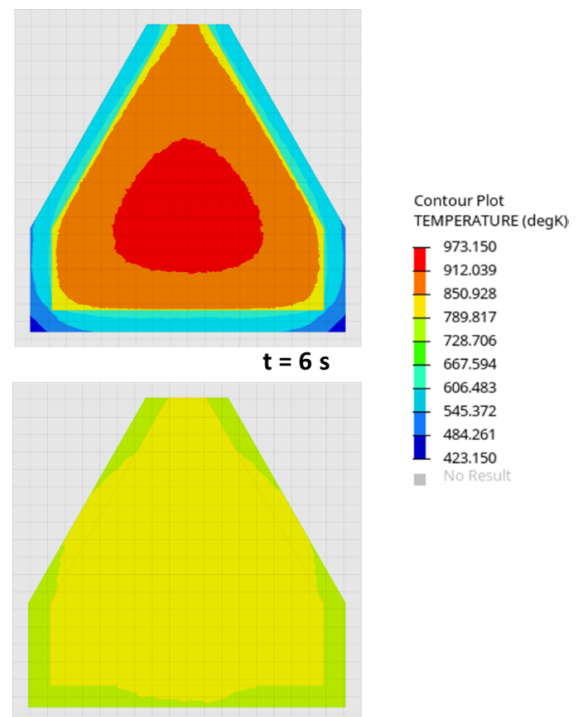


Figure 30. Temperature evolution in the AMS Solver simulation.

Finally, we observe the reported experimental results to compare them to the shrinkage results obtained using the AMS solver. It is important to consider that experimental results are greatly influenced by the material composition, which is normally variable even when considering the same alloy. Also, parameters such as temperature are less accurately controlled in experimental tests, therefore, the results present some deviations among them as shown in Figure 32.



Figure 32. Experimental inner and pipe shrinkage for the Tatur test (left image (Brúna and Sládek 2011); right image (Haj, Bouayad, and Alami 2018)).

In Figure 33 the total shrinkage predicted by the AMS solver is shown. There, we see that the regions where the experimental test shows shrinkage are accurately defined. Height and width are the parameters that appear to be more variable along the different experimental samples. These deviations observed in the samples due to experimental methodology make the comparison, in some cases, very tricky. Although the shrinkage may appear thinner or larger in experimental tests, the main region for a standard AISi9 alloy is accurately determined by AMS.

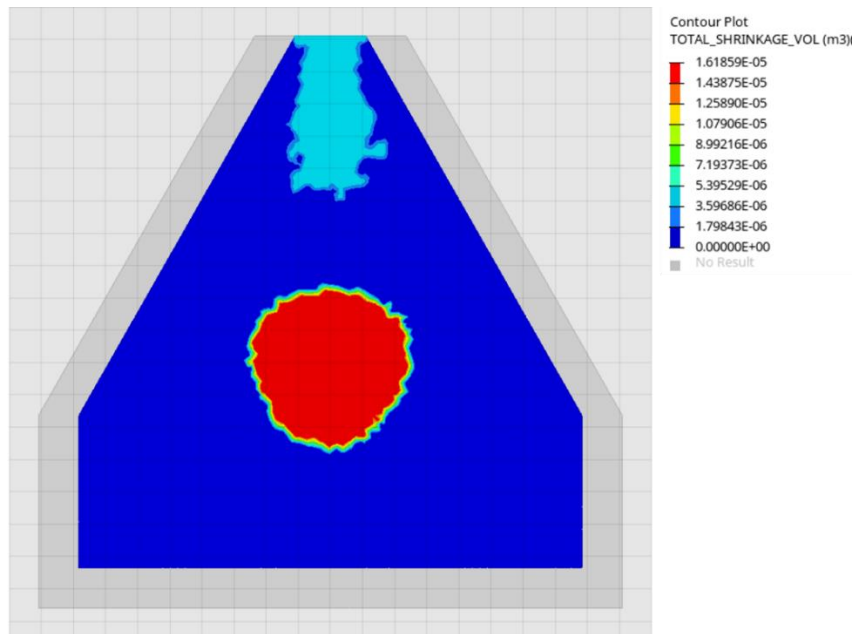


Figure 33. Tatur test total shrinkage result using the AMS Solver.

Finally, Figure 34 shows a quantitative comparison between experimental shrinkage and the solver results. The dispersion of experimental porosity obtained by performing this test presents a deviation of 20%. More accuracy should be reached by considering the average values of more experimental samples.

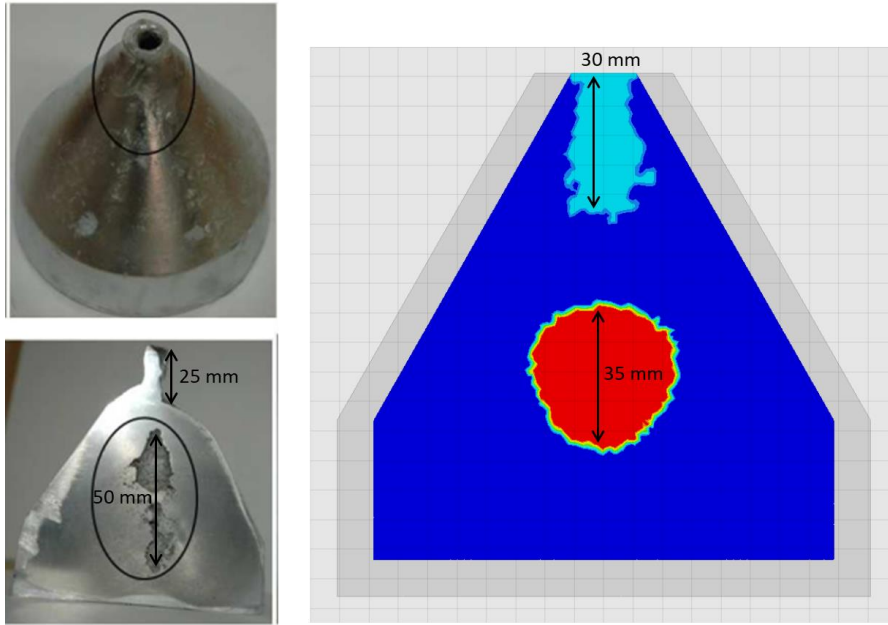


Figure 34. Total shrinkage comparison with experimental results.

Filling Tests

1. Die Filling in Gravity Die Casting: Model 1

Objectives

The present test is carried out with the purpose of evaluating the filling pattern of an aluminum alloy cast with a very simple geometry and based on the work carried out by the authors (Ha et al. 1999). The geometry contains a runner system connected to the cast part with a gate. The test analyzes the flow and velocity of the fluid during filling. The results presented in the reference work compare experimental test to the predictions of simulation softwares. In this benchmark the reported results are compared to the AMS solver predictions.

Method and Description

This test aims to evaluate the filling pattern of an aluminum cast. To replicate the experiment carried out by authors (Ha et al. 1999) This reference geometry is shown in Figure 35, it contains a sprue, a runner system and a gate to connect all the components to the cast part.

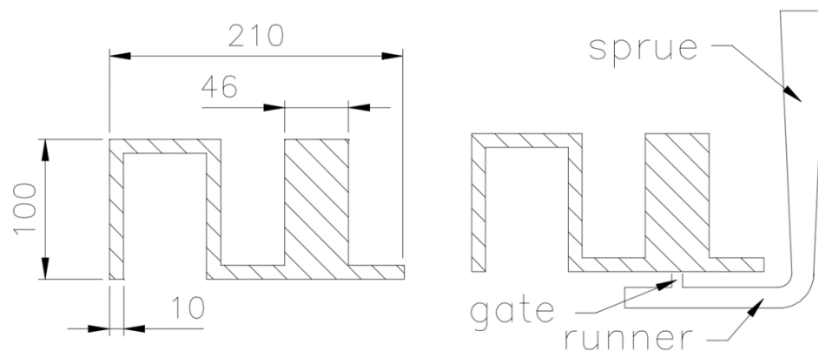


Figure 35. Geometry of the experimental Set-up (Ha et al. 1999).

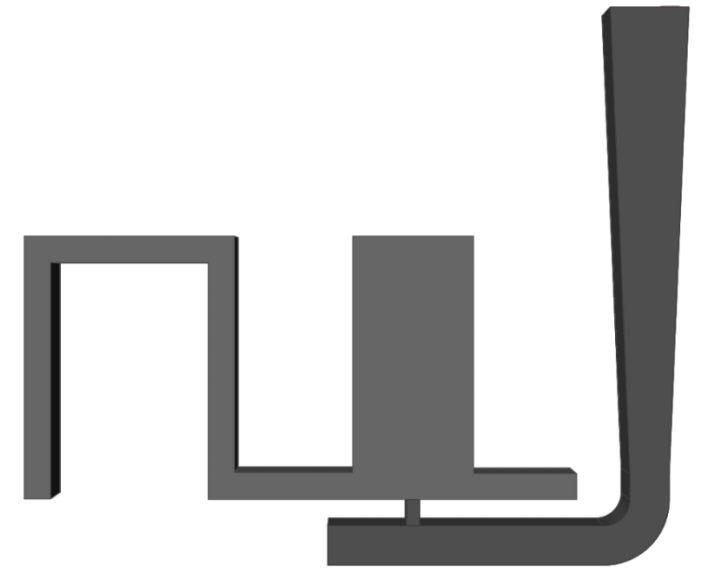


Figure 36. Geometry of the Inspire Cast simulation.

Parameters

MATERIAL DETAILS

The numerical simulations in this experiment are carried out by using the virtual mold feature within the software. The filling is modelled with an ingate of diameter 9mm on top of the sprue and an inlet velocity of 1.02 m/s.

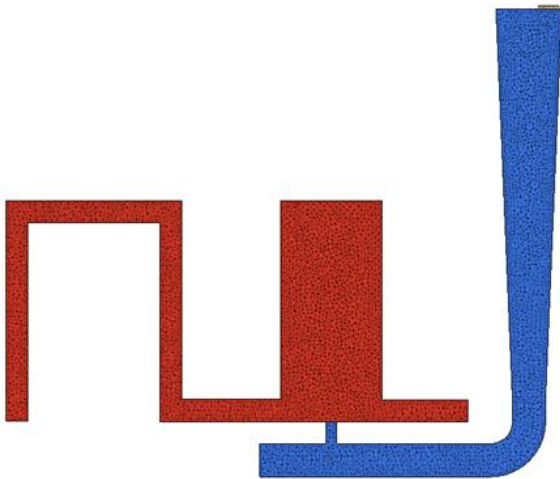
The alloy chosen for the cast part is an aluminum allow A7075 with an estimated initial temperature of 1044.15K. The material properties for this alloy correspond to the default values in the Inspire Cast Data Base.

To avoid solidification during filling, and due to further information available by the authors, the initial temperature for the mold is also 1044.15K.

Component	Material	Initial Temperature (K)
Cast Part	A356	1044.15
Mold	Virtual (1.1730)	1044.15

MESH

To obtain reliable results when analyzing the filling pattern of a model it is crucial to accurately define the mesh size. In this case, the element size is 1.0mm in every component, which generates a mesh of over 1 000 000 elements. It is important to always ensure that the mesh contains at least 3 elements in the narrower region, with this mesh size we reach up to eight elements in the gate which is a tricky region to capture filling behavior.



Component	Size
Cast Part	1.0 mm

Results

We proceed to compare the results of the *AMS solver* simulation to the data available in the literature of reference. In Figure 37 the comparative results are presented, showing the filling pattern and the velocity contour during filling.



Figure 37. Filling (from left to right): AMS Solver, Experimental (Ha et al. 1999), SPH (Ha et al. 1999) and MagmaSoft (Ha et al. 1999).

The results obtained fit with the reported experimental pattern where the filling time is matched very accurately. The filling starts behaving similar to a fountain where a small symmetrical plume is created and spread along the bottom of the mold. The following seconds, the fluid bounces from one side to the other until the principal void is filled, then the flow changes, leading forward to the tale. The free surface during filling also presents a close agreement with experimental and SPH results. As for the MagmaSoft simulation it presents some more differences, mainly in the region of the gate, where the plume is higher and more turbulent.

COARSE MESH

In this section, a coarser mesh is considered to run the same experiment. The new mesh has an element size of 2 mm, this corresponds to the double of the size of the previous test (see Figure 38) and creates a mesh of at least 150 000 elements, this corresponds to a reduction of 85% in relation to the finer mesh. In Figure 39, the results obtained when enlarging element size are compared to the previous results.

In a case like the test proposed, the effect of the mesh size affects directly to the filling pattern due to the number of elements that define the ingate and, therefore, the initial conditions. As the ingate has 9mm diameter, an element size of 2mm is not expected to hide accuracy. It is also ensured that there are at least 6 elements in the width of the gate (the narrower region of the model)

Figure 39 shows that the filling pattern is predicted with accuracy, some differences may be observed in the velocity contour but without mayor incidences. Coarser meshes also tend to increase deviations while trying to replicate the free surface behaviour, considering this effect, Figure 39 shows a good match between results with such different mesh sizes.

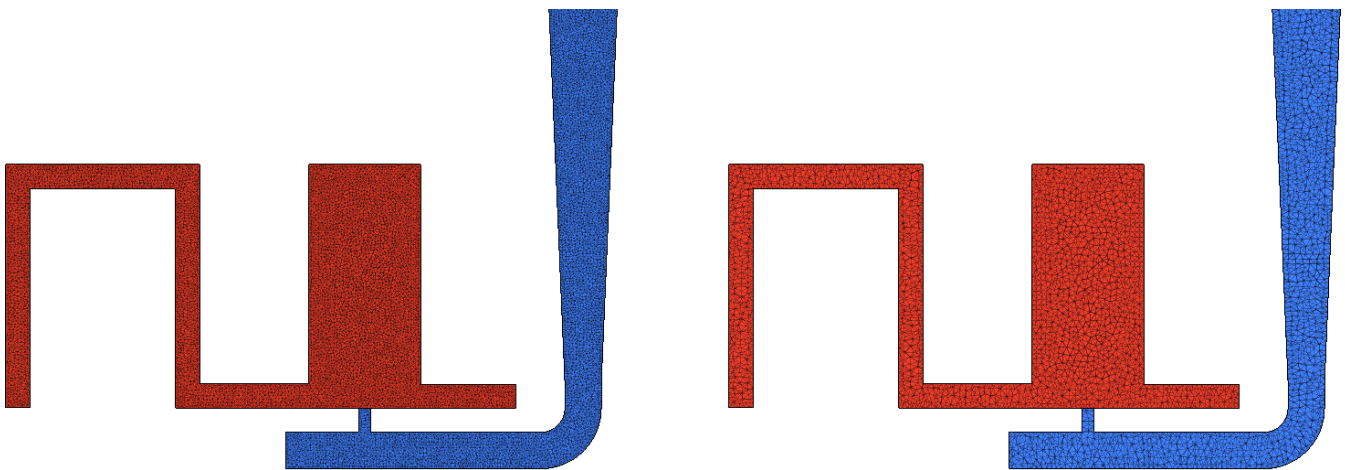


Figure 38. Mesh size: Left) Fine (1mm); Right) Coarse (2mm).

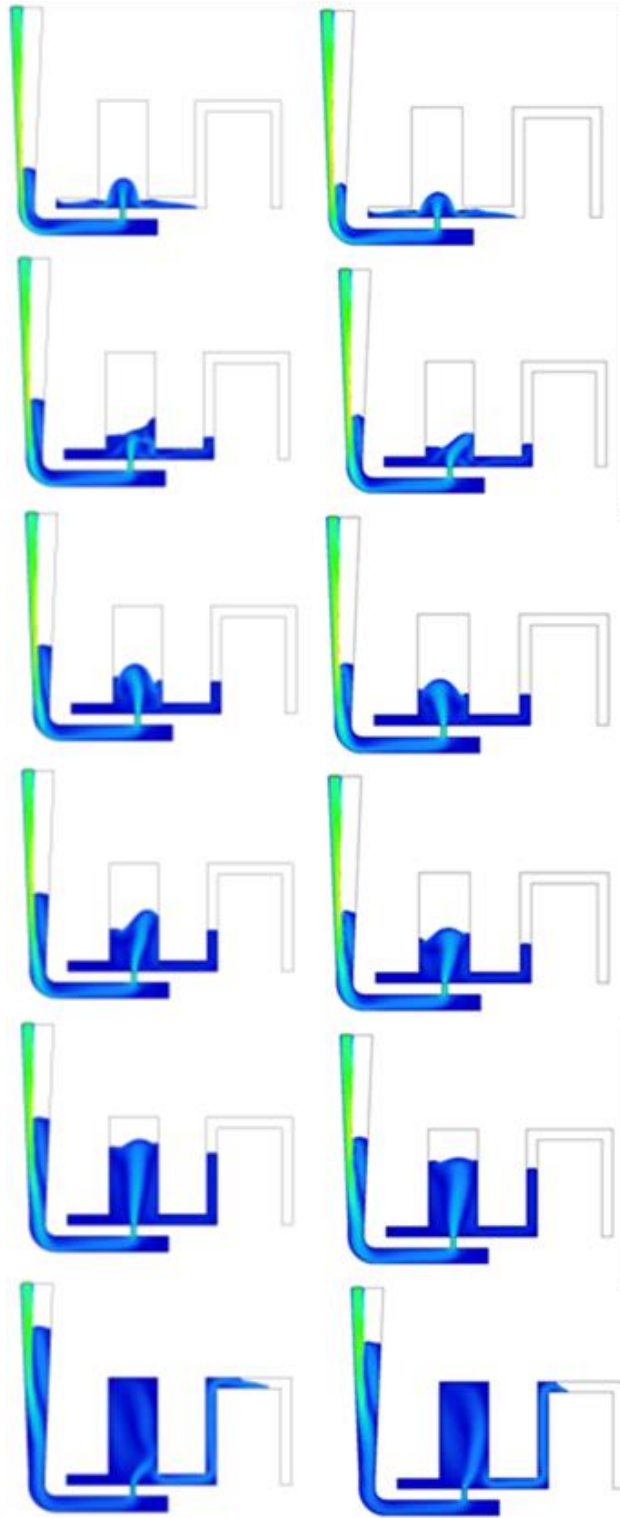


Figure 39. Filling: left) fine mesh (1mm); right) Coarse mesh (2mm)

1. Plunging Jet Test

Objectives

The present test is based by the results obtained in the thesis elaborated by Carl Reilly (Reilly 2010). The main purpose is to evaluate the modelling predictions regarding the filling analysis. To this end, the free surface filling pattern is studied and compared with experimental results and another simulation softwares.

Method and Description

The plunging jet filling test consists in a fine plate with a simple running system as shown in Figure 40. The model is filled using a crucible whose entrance is modelled to act as a stopper at the beginning of the simulation.

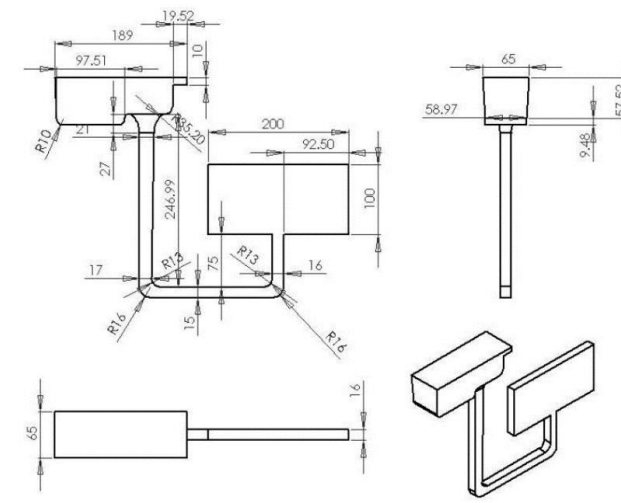


Figure 40. Geometry of the experimental Set-up (Reilly 2010).

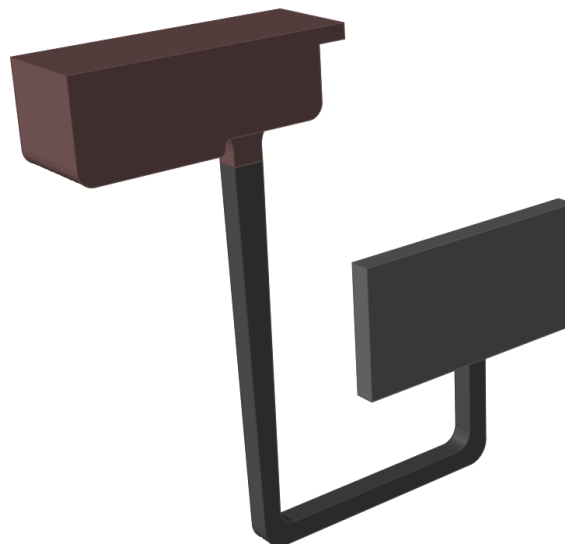


Figure 41. Geometry of the Inspire Cast simulation.

Parameters

MATERIAL DETAILS

The numerical simulations in this experiment are carried out by using the tilting pouring feature within the software. The filling is modelled using a crucible with a very low tilting angle and considerably long tilting time (from $1e-5^\circ$ to 0 in 2.5s). This allows the running system to act as if there was a stopper, as there is in the experimental set up.

The turbulence model uses for the calculation an Smagorinski coefficient of 0.1, which is usually recommended in a range of 0.1-0.18 and defined in the *material.json* file.

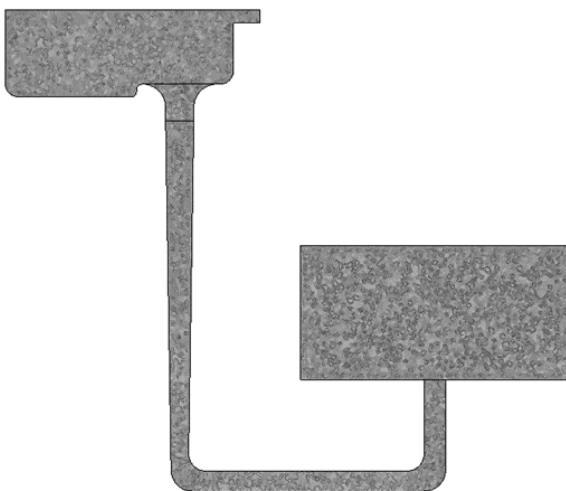
The alloy chosen for the cast part is an aluminum allow A356 with an estimated initial temperature of 991.15K. The dynamic viscosity is considered **2.05e-5 kgm⁻¹s⁻¹**.

The Silica Sand mold presents a heat transfer coefficient to the fluid of **HTC_{Part-Mold}=1500 Wm⁻²K⁻¹** and a thermal conductivity of **0.65Wm⁻¹K⁻¹**. The initial temperature of the mold is 298.00K. Further material properties correspond to the default values in the Inspire Cast Data Base for a Silica Sand mold and for an A356 Aluminum.

Component	Material	Initial Temperature (K)
Cast Part	A356	991.15
Mold	Silica Sand Mold	298.00

MESH

To obtain reliable results when analyzing the filling pattern of a model it is crucial to accurately define the mesh size. In this case, the element size is 1.0mm which generates a mesh of over 1 440 000 elements. It is important to ensure the mesh contains at least three elements in the narrow regions. This mesh size choice allows to reach up to fifteen elements in the gate which is the trickier region in this model when capturing the filling behavior.



Component	Size
Cast Part	1.5 mm
Overflow	1.5 mm
Mold	10.0 mm

Results

We proceed to compare the results of the *AMS solver* simulation to the data available in the literature of reference in which an experimental test was carried out and the X-ray images are reported along with the comparison to a simulation software.

Figure 43 shows the reported experimental results of real time x-rays images of the filling of the casting. In this sequence the air entrapment and fluid front collisions is clearly represented. The bubble formation during filling and folding surfaces phenomena is also noticeable. When comparing this sequence to the one shown in Figure 44(top), obtained modelling the test using AMS simulation solver the results seem to fit with the reported experimental filling pattern. Initially, the incoming fluid jets into the mold cavity, then it falls back directly upon itself under the influence of gravity. This causes high turbulence along with the air entrapment and bubble formation previously mentioned. In both, experimental and simulation models, the flow is broadly symmetrical. Filling time is another parameter that shows good correlation between models, as the filling follows the same time steps as shown in the sequence and at 1.30s volume reached in the plate is very similar.

The modelled results shown in Figure 45 present one clear difference between the experimental results and the AMS simulation results, the jet impacts the roof of the mold, behavior that is no observed in neither of the other tests. This is due to an excess of fluid energy in the Flow3D test which is not representative of the empirical results. Figure 46 shows the velocity contour during filling calculated by AMS, the entrance to the plate is the region where the velocity is increased as it would be expected due to the narrowing and change of pressures.

COARSE MESH

In this section, a coarser mesh is considered to run the same experiment. The new mesh has an element size of 2.5 mm and creates a mesh of at least 310 000 elements. This corresponds to a reduction of 80% in comparison to the finer mesh. In Figure 42, there is a comparison between both meshes. The results obtained when enlarging element size are compared to the previous results. In Figure 44 (bottom) the new calculation of the filling pattern is shown, there are some noticeable different when comparing to the results previously discussed. On the one hand, although the symmetry is well preserved, the turbulence and air entrapment vary significantly decreasing due to the increase in element size. Capturing the filling pattern accurately is highly related to the meshing properties. On the other hand, filling time has also changed, increasing up to 25% in comparison to the finer mesh (plate with fine mesh fills in 1.5s and with coarser mesh reaches 2.0 s) and the volume contained in the plate in the last time step shown in the sequence reinforces this result. .

In a case like the test proposed, the effect of the mesh size affects directly to the filling pattern as described. Coarser meshes also tend to increase deviations while trying to replicate the free surface behavior which is also related with the decreased certainty in the turbulence performance and bubble appearance.

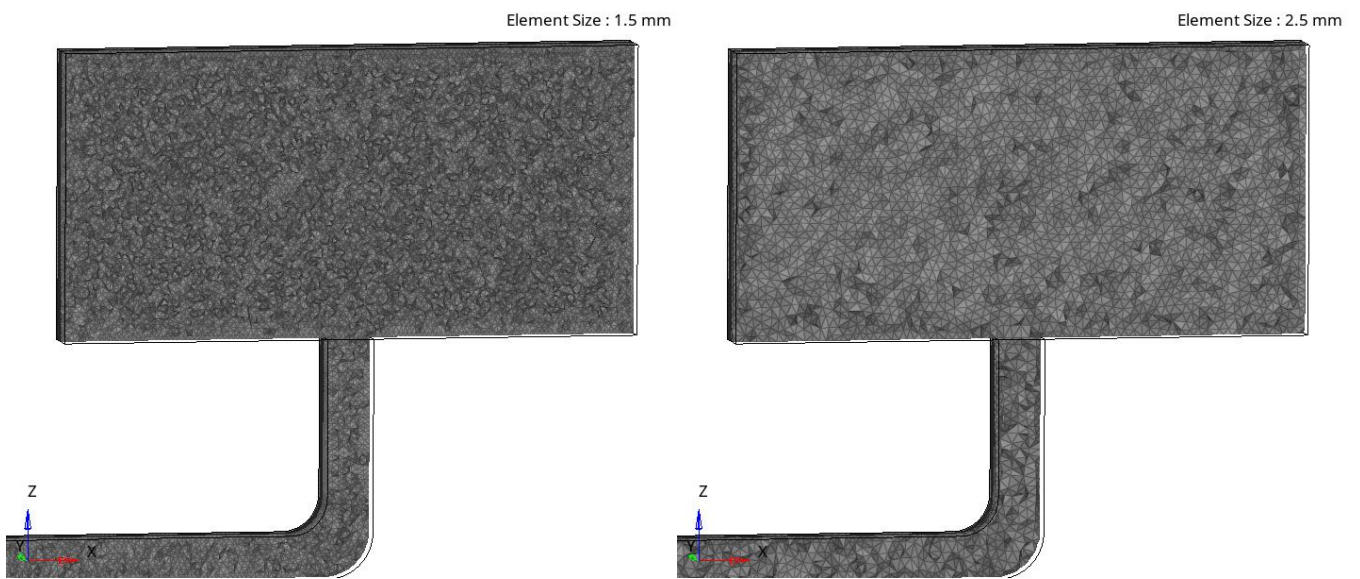


Figure 42. Mesh size: Left) Fine (1.5mm); Right) Coarse (2.5mm).

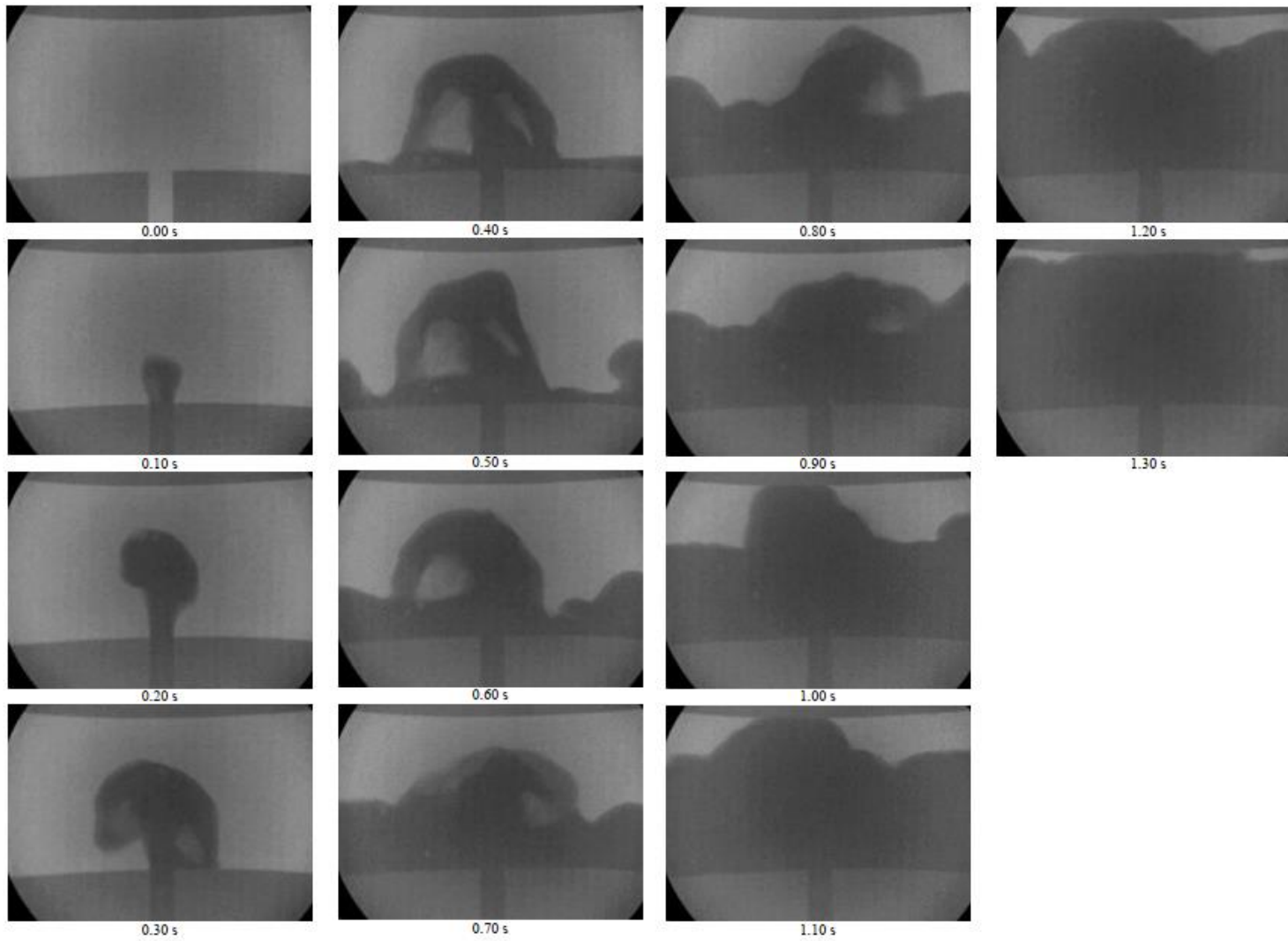


Figure 43. Experimental filling pattern (Reilly 2010).

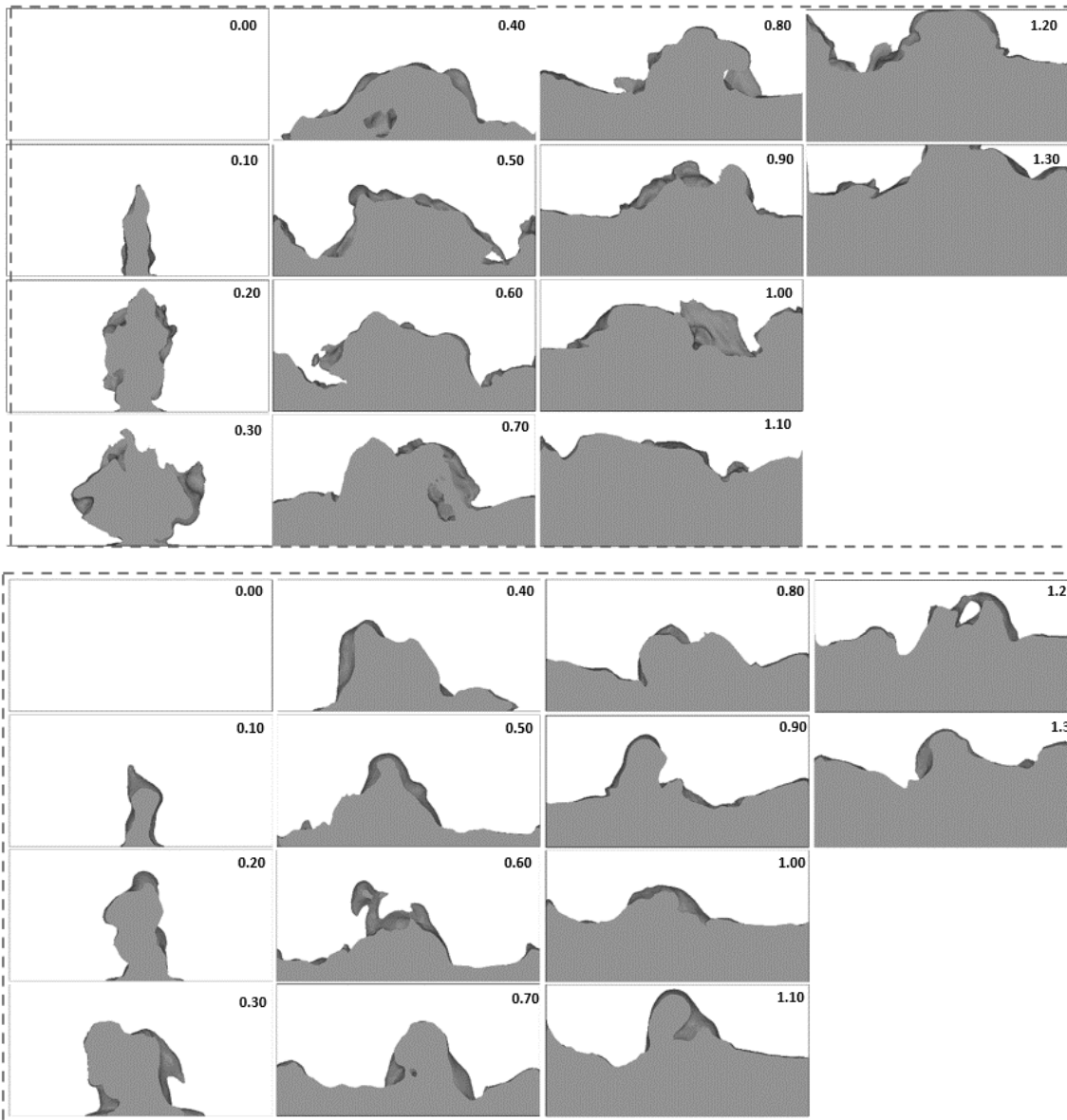


Figure 44. Filling pattern results (AMS):
 Top) Fine mesh ; Bottom) Coarse Mesh

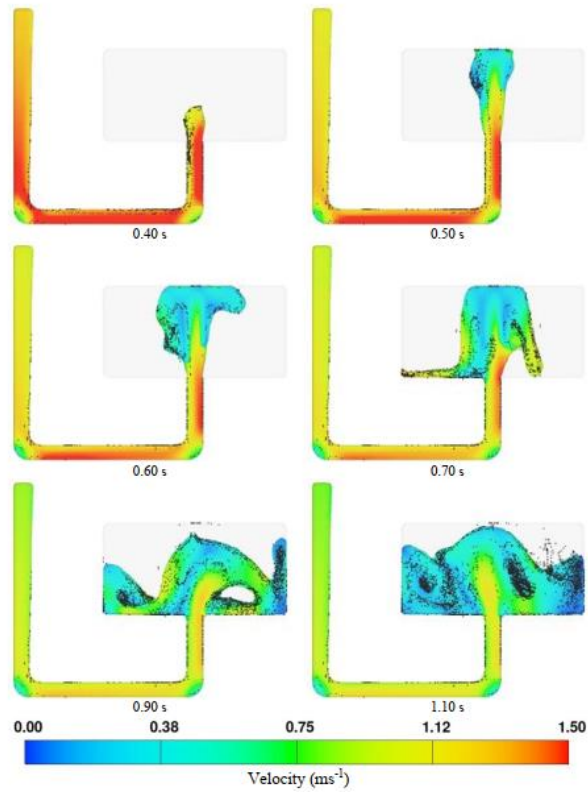


Figure 45. Filling results (Flow3D) (Reilly 2010).

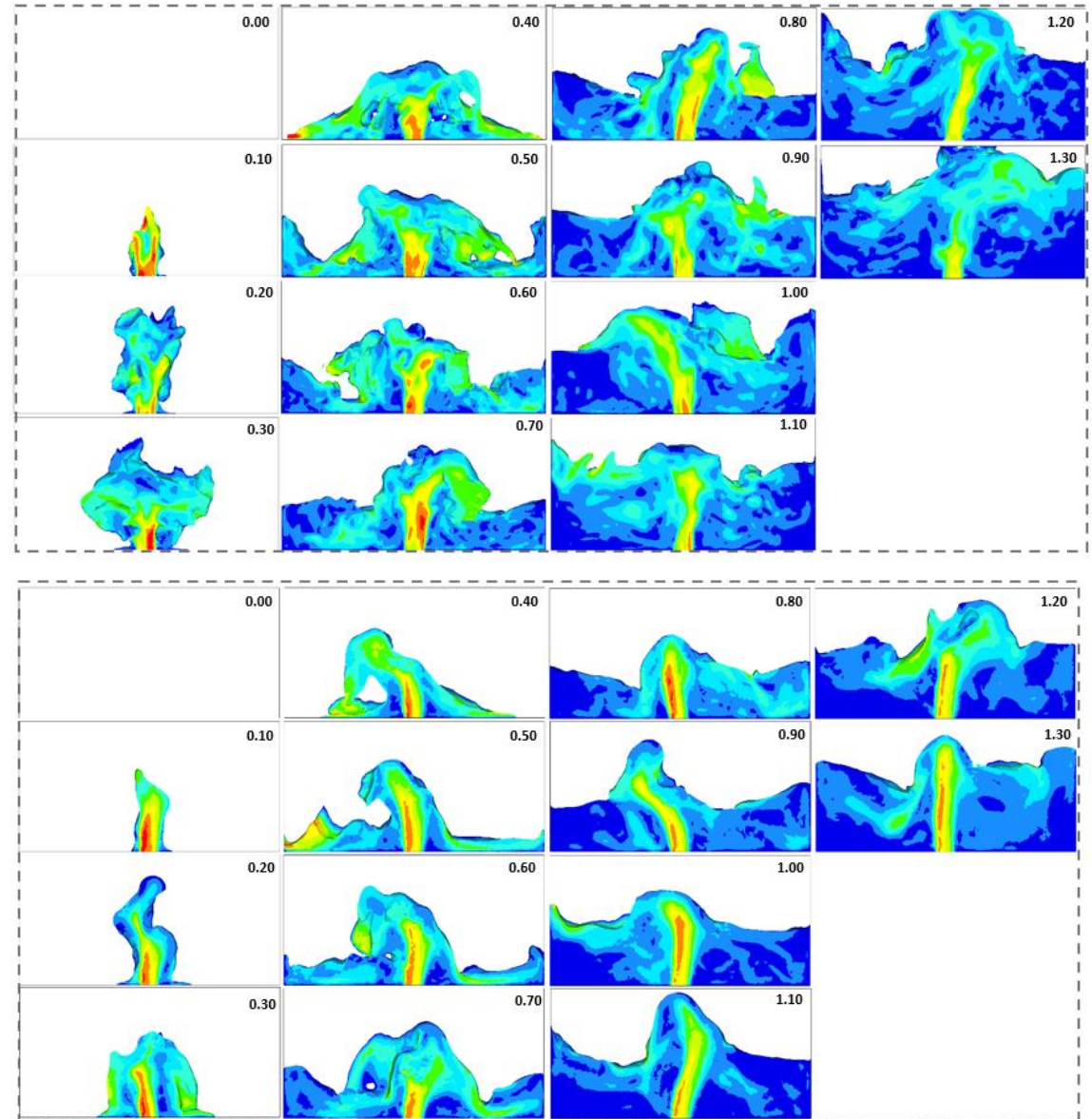


Figure 46. Velocity contour (AMS): Top
Fine mesh ; Bottom) Coarse Mesh

References

- Brůna, M., A. Sládek, and L. Kucharčík. 2012. "Formation of Porosity in Al-Si Alloys." *Archives of Foundry Engineering* 12 (1): 5–8. <https://doi.org/10.2478/v10266-012-0001-5>.
- Brůna, M, and A Sládek. 2011. "Hydrogen Analysis and Effect of Filtration on Final Quality of Castings from Aluminium Alloy AlSi7Mg0,3." *Archives of Foundry Engineering* 11 (1): 5–10.
- Carlson, Kent D, and Christoph Beckermann. 2009. "Prediction of Shrinkage Pore Volume Fraction Using a Dimensionless Niyama Criterion" 40 (JANUARY): 163–75. <https://doi.org/10.1007/s11661-008-9715-y>.
- Chiumenti, Michele, Miguel Cervera, and Emilio Salsi. 2018. "A Phenomenological Model for the Solidification of Eutectic and Hypoeutectic Alloys Including Recalescence and Undercooling." *Journal of Heat Transfer*, no. June. <https://doi.org/10.1115/1.4039991>.
- Chouchane, Mnaouar, Tahar Fakhfakh, Hachmi Ben Daly, Nizar Aifaoui, and Fakher Chaari. 2015. "Design and Modeling of Mechanical Systems - II: Proceedings of the Sixth Conference on Design and Modeling of Mechanical Systems, CMSM 2015 March 23-25, Hammamet, Tunisia." *Lecture Notes in Control and Information Sciences* 789: 297–303. <https://doi.org/10.1007/978-3-319-17527-0>.
- Ha, Joseph, Paul Cleary, Vladimir Alguine, and Thang Nguyen. 1999. "SIMULATION OF DIE FILLING IN GRAVITY DIE CASTING USING SPH AND MAGMASoft," no. December: 423–28.
- Hag, Badiâ Air El, Aboubakr Baouayad, and Mohammed Alami. 2015. "A Comparison between Numerical Simulation and Experimental Determination of Porosity." *Design and Modeling of Mechanical Systems, Lecture Notes in Mechanical Engineering*, II. https://doi.org/10.1007/978-3-319-17527-0_29.
- Haj, B A I T E L, A Bouayad, and M Alami. 2018. "Quantitative Evaluation of Shrinkage Porosity in AlSi9" 8 (6): 365–72.
- Hajkowski, J., P. Roquet, M. Khamashta, E. Codina, and Z. Ignaszak. 2017. "Validation Tests of Prediction Modules of Shrinkage Defects in Cast Iron Sample." *Archives of Foundry Engineering* 17 (1): 57–66. <https://doi.org/10.1515/afe-2017-0011>.
- Kron, J, M Bellet, A Ludwig, B Pustal, J Wendt, H Fredriksson, M Bellet, et al. 2017. "Comparison of Numerical Simulation Models for Predicting Temperature in Solidification Analysis with Reference to Air Gap Formation Comparison of Numerical Simulation Models for Predicting Temperature in Solidification Analysis with Reference to Air Gap F" 0461 (July). <https://doi.org/10.1179/136404604225020669>.
- Laschet, Gottfried, Jürgen Jakumeit, and Stefan Benke. n.d. "Thermo-Mechanical Analysis of Cast / Mould."
- Reilly, C. 2010. "Development of Quantitative Casting Quality Assessment Criteria Using Process Modelling," no. March: 563.